University of Szeged

Faculty of Pharmacy

Institute of Pharmaceutical Technology and Regulatory Affairs

INCREASING THE OPHTHALMIC BIOAVAILABILITY USING INNOVATIVE DRUG DELIVERY SYSTEMS

Ph.D. Thesis

L.Kiss Eszter, Pharm. D.

Supervisor:

Erzsébet Csányi, Pharm.D., Ph.D., dr.habil.

Budai-Szűcs Mária Pharm.D., Ph.D., dr.habil.

2021

PUBLICATIONS RELATED TO THE SUBJECT OF THE THESIS

I. Mária, Budai-Szűcs; **Eszter, L Kiss**; Barnabás, Áron Szilágyi; András, Szilágyi; Benjámin, Gyarmati; Szilvia, Berkó; Anita, Kovács; Gabriella, Horvát; Zoltán, Aigner; Judit, Soós and Erzsébet Csányi; Mucoadhesive Cyclodextrin-Modified Thiolated Poly(aspartic acid) as a Potential Ophthalmic Drug Delivery System. Polymers 10, 199 (2018).

IF: 3.164

II. **Eszter, L. Kiss**; Szilvia, Berkó; Attila, Gácsi; Anita, Kovács; Gábor, Katona; Judit, Soós; Erzsébet, Csányi; Ilona, Gróf; András, Harazin; Mária A., Deli, and Mária, Budai-Szűcs; Design and Optimization of Nanostructured Lipid Carrier Containing Dexamethasone for Ophthalmic Use. Pharmaceutics 11, 679 (2019).

IF: 4.421

III. **Eszter, L. Kiss**; Szilvia, Berkó; Attila, Gácsi; Anita, Kovács; Gábor, Katona; Judit, Soós; Erzsébet, Csányi; Ilona, Gróf; András, Harazin; Mária A., Deli, György T. Balogh and Mária, Budai-Szűcs; Development and Characterization of Potential Ocular Mucoadhesive Nano Lipid Carriers Using Full Factorial Design. Pharmaceutics 12, 682 (2020).

IF: 4.421

ABSTRACTS RELATED TO THE SUBJECT OF THE THESIS

I. **Eszter, L. Kiss**; Mária, Budai-Szűcs; Áron, Szilágyi Barnabás; András, Szilágyi; Benjámin, Gyarmati; Erzsébet, Csányi: Cyclodextrin-Modified Thiolated Poly(aspartic acid) as a Potential Mucoadhesive Ophthalmic Drug Delivery, 4th International Conference on Bio-Based Polymers and Composites, Balatonfüred, Hungary, 2018.09.02-06. (Verbal presentation)

II. **Eszter, L Kiss**; Barnabás, Szilágyi; András, Szilágyi; Benjamin, Gyarmati; Erzsébet, Csányi; Mária, Budai-Szűcs: Cyclodextrin-Modified Mucoadhesive Polymers as an Enhancer of Ophtalmic Drug Delivery, 12th Central European Symposium on Pharmaceutical Technology and Regulatory Affairs, Szeged, Hungary, 2018.09.20-22. (Poster presentation)

III. **Eszter, L. Kiss**; Mária, Budai-Szűcs; Erzsébet, Csányi: Improving the ophthalmic bioavailability of steroidal anti-inflammatory drugs, I. Symposium of Young Researchers on Pharmaceutical Technology, Biotechnology and Regulatory Science, Szeged, Hungary, 2019.01.31. (Verbal presentartion)

IV. **Eszter, L. Kiss**; Szilvia, Berkó; Anita, Kovács; Attila, Gácsi; Mária, Budai-Szűcs; Erzsébet, Csányi; Dexametazon tartalmú nanostrukturált lipid hordozók preformulációs és formulációs vizsgálatai; Gyógyszertechnológiai és Ipari Gyógyszerészeti Konferencia: A Magyar Gyógyszerésztudományi Társaság Gyógyszeripari Szervezetének és Gyógyszertechnológiai Szakosztályának Konferenciája, Siófok, Hungary, 2019.09.26-28. (Poster presentation)

V. **Eszter, L. Kiss**; Erzsébet, Csányi; Mária, Budai-Szűcs; Nanostructured lipid carriers for ophthalmic use, II. Symposium of Young Researchers on Pharmaceutical Technology, Biotechnology and Regulatory Science, Szeged, Hungary, 2020.01.23-24. (Verbal presentation)

VI. **Eszter, L. Kiss**; Erzsébet, Csányi; Mária, Budai-Szűcs; Mucoadhesive nanostructured lipid carriers for ophthalmic use, III. Symposium of Young Researchers on Pharmaceutical Technology, Biotechnology and Regulatory Science, Szeged, Hungary, 2021.01.20-22. (Verbal presentation)

Table of contents

ABBREVIATIONS

API	active pharmaceutical ingredient
CD	cyclodextrin
CI%	crystallinity index
DXM	dexamethasone
EE %	entrapment efficiency
G’	storage modulus
G’’	loss modulus
HCE-T cells	Human corneal epithelial cell-transformed
k’	stability constant
LM	lipid mixtures
MABCD	6-monodeoxy-6-monoamino-beta-cyclodextrin hydrochloride
MABCD-PR	monoamino-β-cyclodextrine prednisolone complex
MTT	3-(4,5-dimethylthiazol-2-yl)-2,5-diphenyltetrazolium bromide
PAMPA	parallel artificial membrane permeability assay
PASP	poly(aspartic acid)
PASP-CEA	thiolated poly(aspartic acid)
PASP-CEA-CD	cyclodextrin functionalized thiolated poly(aspartic acid)
PASP-CEA-CD-PR	PASP-CEA-CD and PR complex
PDI	polydispersity index
PR	prednisolone
TEER	transepithelial electrical resistance
XRPD	X-ray powder diffractometer
Z_{ave}	hydrodynamic diameter
ZP	zeta potential

1. INTRODUCTION

There is an increasing global need to develop new non-invasive ophthalmic treatments as there are many poorly understood and sometimes incurable vision-threatening diseases and conditions. The most common ocular diseases are glaucoma, infections, dry eye syndrome, allergies, corneal neovascularization, corneal erosion, inflammation, and macular degeneration. Most of the current treatments are mainly limited to conventional medicines, and in many cases, the treatment only affects the symptoms of the disease, not the underlying cause. Currently, advanced ophthalmic therapies do not just have to mean to treat various eye diseases but also have to be able to improve patient compliance or restore the healthy state of the eye. Topical ophthalmic treatments are considered the safest and the least invasive therapies, and they are easy to handle for patients. However, due to their low bioavailability, there is a great need for their development. There are several difficulties to the successful and effective delivery of the active ingredient to the eye. These include, for example, limiting factors due to the anatomical complexity and biopharmacy of the eye, and challenges related to patient compliance, e.g. inconvenience of frequent usage. Consequently, these aspects, in any case, should be taken into account when developing a new ophthalmic drug delivery system[1].

In recent technological developments, there are three main strategies to achieve the above-mentioned goals. In one case, the residence time of the preparation on the surface of the eye is increased. In another case, the carrier contains the active ingredient in such a form that it is already suitable for permeation (increased solubility). In the third case, the penetration of the drug is improved. During the course of my Ph.D. research, the development of delivery systems was in line with the above-mentioned strategies.

2. LITERATURE BACKGROUND

2.1. Challenges in ocular drug delivery

Anatomically, the eyeball can be divided into anterior and posterior segments. The anterior segment includes the cornea, conjunctiva, iris, ciliary body, tear film, chambers. The posterior segment includes the retina, choroid, sclera, vitreous body, and Bruch membrane (Fig.1.).[2]

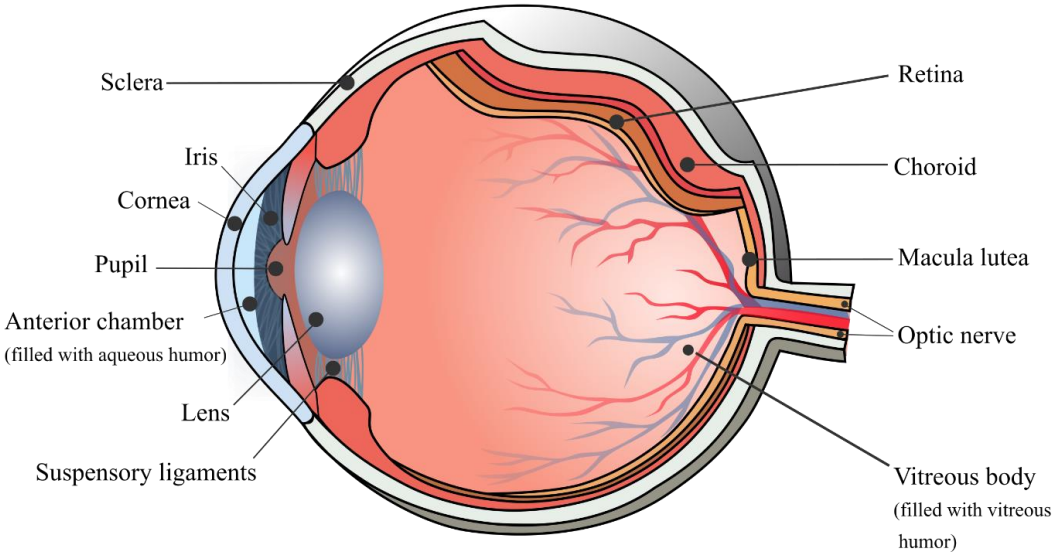

Figure 1. *Anatomy of the eye*

Whether the application is local or systemic, to achieve the intended effect, the drug needs to get through the static, dynamic, and metabolic barriers of the eye in both the anterior and posterior segments. Static barriers include the different layers of the cornea, the sclera, and the iris/ciliary muscle, which acts as a barrier between blood and aqueous humor. The retina also counts as a static barrier but acts as a barrier between blood and the retina. Dynamic barriers include the tear film, the retinal and conjunctival blood flow, and the lymph flow. In addition, various efflux pumps also prevent contact with active ingredients, for example, P-glycoproteins (P-gp) and multidrug-resistant proteins (MRP). Most of these functions regulate the inward and/or outward moving of molecules in the capillaries of the eye, similar to the functions of the blood-brain barrier. [3,4].

When targeting the deeper layers of the eye in topical therapy, it is generally expected that the appropriate physical properties (molecular weight, pH, hydrophilicity, and lipophilicity), as well as adequate ophthalmic tolerability, should be ensured for any dose of the active ingredient. However, ophthalmic systems applied topically to the surface of the eye, nearly 90% of which are eye drops, do not meet these criteria.

It is a known fact that a tight occluding corneal epithelium controls the permeation of the drug into the anterior segment of the eye. A significant portion of the molecules that have already penetrated are also washed out due to blood flow and tearing within the choroid, ciliary body, or iris. As a result, a very small proportion of the active ingredients, which are applied to the surface, reach the posterior segment of the eye. In order to exceed these deficiencies, ophthalmic drugs e.g. anti-glaucoma agents, corticosteroids and certain antibiotics need to be administered systemically [1,5].

2.2. Nano ophthalmic formulations

Nanoparticles with proper formulation in both ways, i.e. by increasing residence time on the eye and increasing penetration, it is possible to increase the bioavailability of the drug, so nanosystems can target the anterior and posterior segments of the eye with topical application.

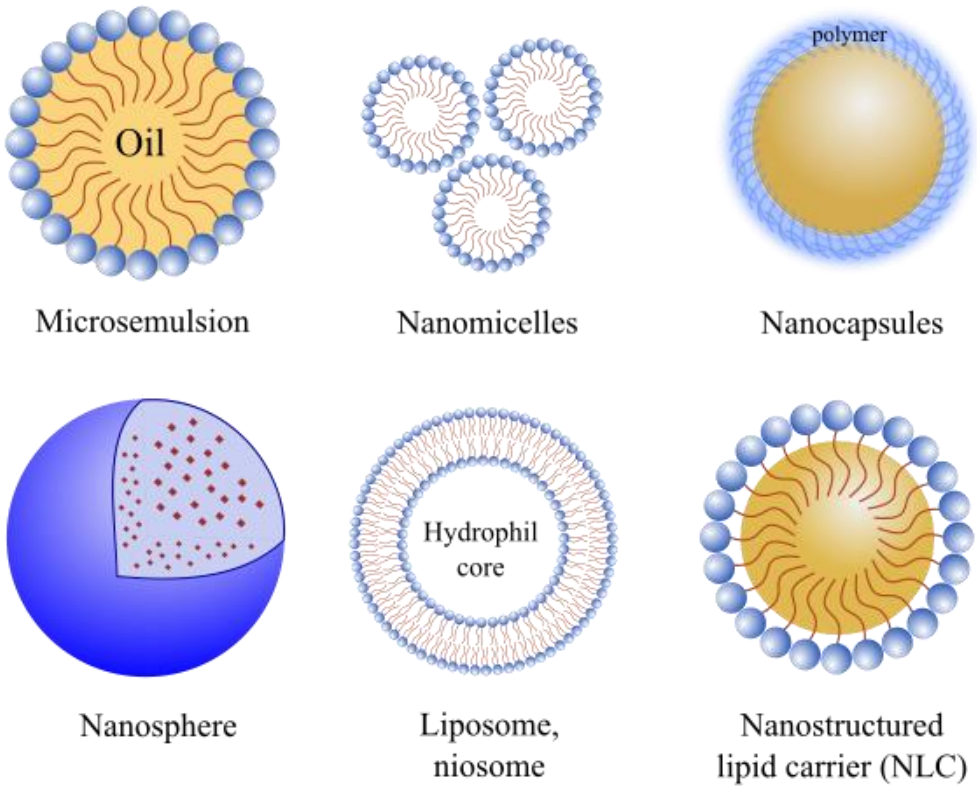

***Figure 2**. Nanostructured carriers*

Nowadays, more and more ophthalmic nano-drug delivery strategies are emerging[6] (Fig. 2.). Lipid-based nanocarriers have a number of potential benefits, such as improving the bioavailability of poorly water-soluble drugs; ensuring targeted and controlled drug release, resulting in a reduction in side effects [2]. In

addition, they increase the residence time on the eye and the penetration through the cornea[7].

Ophthalmic microemulsions consist of an oily inner phase, a surrounding emulsifying layer and an outer aqueous phase. Their advantages include transparency, thermodynamic stability, and high solvation capacity. Due to their emulsifier content, they increase the permeability of the membranes, thus the diffusion of the active ingredient into the deeper layers of the eye. Their disadvantage may be that they can irritate the conjunctiva due to the high emulsifier content [8,9].

Nanomicelles are one of the most commonly used ophthalmic nanoscale drug delivery systems suitable for treating both anterior and posterior segments. A self-assembling nanomicelle can be easily created with amphoteric molecules, and used safely due to its small excipient content. The hydrophobic core and hydrophilic shell allow the encapsulation of hydrophobic molecules in a clear, transparent aqueous medium[10]. For example, dexamethasone, which is a steroidal anti-inflammatory drug, is used in a nanomicellar system to achieve better bioavailability than in a conventional suspension form [6,11].

The two main groups of nanoparticles are nanocapsules and nanospheres, both of which are composed primarily of natural or synthetic polymers, lipids, or proteins. In the case of nanocapsules, the core, which also contains the internal drug, is coated with a polymeric membrane that controls drug release. However, in nanospheres, the drug is uniformly distributed in a matrix. In the case of the latter, due to homogenous distribution, mild mucosal irritation can also be expected. Another advantageous feature of nanospheres is that they can be easily resized between tens and hundreds of nanometers. They have good bioavailability and biocompatibility, which have been confirmed by several studies[12,13].

Some examples of polymer-based nanocarriers in ophthalmology can be found in the literature: for example, progesterone-containing poly(butyl cyanoacrylate) nanospheres[14]; and albumin and chitosan nanoparticles were also studied. Due to their cationic properties, the latter is strongly bound to the cornea by ionic interactions, so their advantageous properties can also be exploited in the treatment of the ocular surface[15]. Polymer-based but less mucoadhesive nanosystems can also be coated with a polymer with better adhesion to increase mucoadhesion (e.g., coating indomethacin with poly-ε-caprolactone with chitosan[16].

Liposomes are spherical lipid vesicles composed of a hydrophilic inner phase enclosed by one or more phospholipid bilayers with different properties based on

their chemical composition. Their advantages include good biocompatibility, bioavailability, better selectivity, and the ability to encapsulate both hydrophobic and hydrophilic drugs[6]. An example of this is that tacrolimus, which is used to treat uveitis, incorporated into liposome in order to reduce the side effects[6,17].

Nanostructured lipid carriers (NLC) as lipid nanoparticles are potential drug delivery systems that have several advantages in ophthalmic therapy. NLCs as drug delivery systems may be alternatives to microemulsions or liposomes because they have a small particle size (50–400 nm) while having a lower emulsifier concentration[18,19]. Compared to SLNs, NLCs can provide higher encapsulation efficiency due to their low crystallinity index. They may increase corneal penetration in a non-invasive manner leading to higher ophthalmic bioavailability and patient compliance[20]. In addition, the potential mucoadhesive nature of NLCs may improve interaction with the corneal membrane, resulting in longer residence time, increased bioavailability, and reduced possible side effects.

Several research groups have published their work on the ophthalmic NLCs, including examples of developments in the treatment of inflammation, infections, glaucoma, and other disorders affecting the posterior segment of the eye[20]. Ibuprofen[21], flurbiprofen[22], indomethacin[23] as non-steroidal anti-inflammatory drugs, and triamcinolone acetonide (TA)[24] and dexamethasone[25] as steroidal anti-inflammatory drugs were incorporated into NLC systems. Based on the literature data, these NLCs can also be used to treat the anterior and posterior segments of the eye[21,22].

Araújo et. al. encapsulated TA into NLCs in order to increase its eye bioavailability. TA is a corticosteroid drug, currently administered by intravitreal injection for the treatment of a broad spectrum of inflammatory, oedematous and angiogenic eye diseases. Nanometric (~200 nm), unimodal and negatively charged NLCs were developed to deliver the lipophilic TA through the cornea and the non-cornea to the back segment of the eye. The results showed a quite stable particle size with a low tendency of particle aggregation during the storage[24].

Nanosuspensions are nanosized particles in which the active ingredients form a kind of colloidal dispersed system. These systems can improve the retention time and bioavailability of lipophilic drugs[6]. The use of corticosteroids (such as prednisolone, dexamethasone, and hydrocortisone) in nanosuspension can reduce the therapeutic dose, which enables to avoid the potential side effects of high doses such as cataracts, glaucoma, and optic nerve damage[26,27].

2.3 Hydrogels as innovative ocular drug delivery systems

Hydrogels are crosslinked polymer networks that are capable of absorbing large amounts of water or other biological fluids due to the presence of hydrophilic groups within the porous polymer structure. They can be composed of both natural and synthetic polymers by chemical or physical crosslinking[28–30]. The most important properties of hydrogels are hydrophilicity, flexibility, elasticity, and high water content. All these properties make them widely suitable in various fields of biomedical science. In general, hydrogels show high compatibility with biological systems, and even their soft nature minimizes irritation and foreign body sensation to the surrounding tissues[31–33].

So-called smart hydrogels are sensitive to external stimuli and their environment, so they respond to the resulting physical, chemical or biological stimuli by volume change, or phase transition. *In situ* gel formation can be of paramount importance in ophthalmic topical therapy, both on the surface of the eye and as an intravitreal injectable system. In situ gelling eyedrops can be easily spread as a liquid and provide long-term effectiveness on the eye surface after gelling. Intravitreal injectable systems can form a depot in the vitreous body after injection.

Signals or stimuli that induce structural changes in intelligent polymers can be divided into three main groups: physical (temperature, ultrasound, light or mechanical stress), chemical (pH, ionic strength and redox potential) and biological (enzymes and other biomolecules)[34]. These signals or stimuli can be artificially controlled (e.g., by a magnetic or electric field using light or ultrasound); or triggered by the internal physiological environment. Such internal physiological conditions or their changes (e.g., in pathological conditions) may include, for example, pH, or changes in certain vital organs; or in connection with a disease, a change in the temperature, the presence of enzymes or other antigens. Ophthalmic *in situ* gelling systems are viscous liquids that spread easily after instillation and then gel is formed upon environmental stimuli. The formed gel layer resists elimination mechanisms, however, the associated mucoadhesive nature enhances ocular surface retention [35].

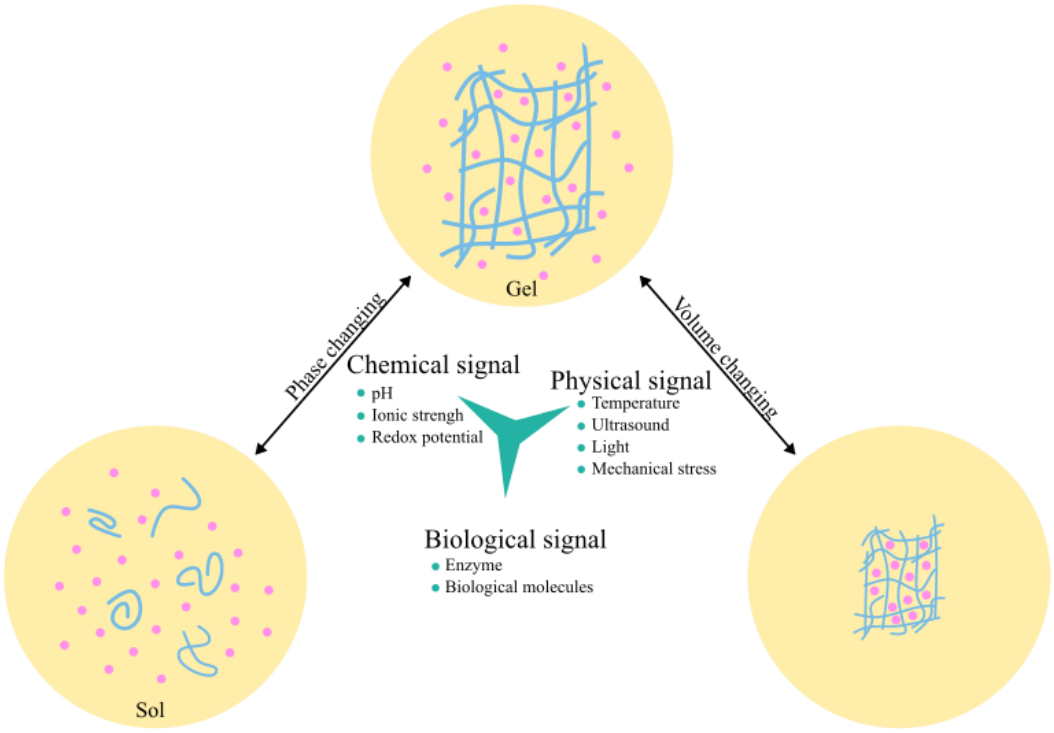

***Figure 3**. The phase and volume change of hydrogels*

On the surface of the eye, several stimuli can be used which can lead to *in situ* gelation (Fig. 3.), but in all cases the time-dependency of the sol-gel transition in systems should be considered a critical parameter. Too fast gelation can be detrimental to ocular surface distribution, and too slow gelation can lead to premature leaching and dilution, which can be a barrier to gelation. In general, ophthalmic systems can use four types of stimulus-sensitive polymers: thermo-sensitive, pH-sensitive, ion-activated, and more recently, redox potential sensitive polymers.

Thermosensitive intelligent polymers are sensitive to temperature: microstructural changes occur, associates are formed, which result in a gel structure. In ophthalmic formulations, the most commonly used heat-sensitive polymers are poloxamers, xyloglucans, poly-N-isopropyl acrylamide, and chitosans[36].

Chitosan is an aminopolysaccharide that is useful in medical practice due to its good biocompatibility. It is biodegradable and has low cytotoxicity. As mentioned earlier, because of its positive charge, chitosan adheres well to the negatively charged surface mucin layer of the eye[37]. In 2000, Chenite et al. developed an injectable, thermo-sensitive, pH-dependent solution based on neutralization by the addition of chitosan β-glycerol phosphate[38]. The resulting solution is a reversibly thermo-sensitive polymer that forms a liquid at room temperature but gels at body temperature[39], thus providing an *in situ* gelation[40].

Significant variations in pH can be observed in different parts and states of the human body. That is why pH can be used in therapeutic systems that may be specific for certain

body surfaces, tissues, or intracellular matrices. Due to the large variations of pH values in physiological fluids, sol-gel transitions induced by pH changes are an ideal solution to enhance the pharmacological effects of topical drug delivery, especially for ophthalmic applications[41]. Polyelectrolytes as pH-sensitive polymers are capable of binding acidic (carboxylic acid or sulfonic acid) or basic groups (ammonium salts), or releasing protons in response to changes in environmental pH[35]. The most common pH-sensitive polymers in ophthalmic formulations are polyacrylic acid, polycarbophil, chitosan, and cellulose acetate phthalate[35].

In ion-sensitive polymers, phase transitions occur under the influence of various electrolytes. Various electrolytes in the tear fluid promote the sol-gel transition of certain polymers, thereby increasing the ocular residence time and bioavailability of the drug. Examples of such polymers are kappa-carrageenan and gellan gum, which can interact with cations such as Na^+, K^+, Mg^{2+}, Ca^{2+} [42].

Redox-sensitive thiolated polymers (thiomers) are mucoadhesive polymers with a thiol-containing side chain. The most commonly used thiomers have been synthesized from chitosan, alginate, polyacrylate, and cellulose derivatives[43]. In addition to *in situ* gelation, they are able to form covalent (disulfide) bonds with cysteine-rich domains of the ocular surface mucin[44]. As a result, both the residence time on the mucosa and thus bioavailability can increase.

2.4. Combination of hydrogels and nanocarriers

In recent years, a number of papers have been published in which nanocomposites (nanoparticles[45], nanoemulsions[46], niosomes[47]) were combined with hydrogels in order to further increase the ophthalmic bioavailability of the active ingredients. In nano-hydrogel hybrid systems, carbopols, chitosans, hypromellose, and natural gums were the most commonly used polymers.

Yu et al. prepared liposomes containing timolol maleate and placed them in a gellan gum gel. This combination prolonged the duration and shortened the time required for the pharmacological effect[48]. Lux et al. developed a lyophilized polymer matrix from hypromellose which was mounted on a flexible polytetrafluoroethylene carrier tape. Upon contact with the conjunctiva, the tear film rapidly hydrated the pattern. Compared to conventional eye drops, this new route of administration resulted in significantly higher corneal and aqueous humor concentrations seven hours after application[49].

Morsi et al. prepared an acetazolamide-containing nanoemulsion formulation by incorporating a combination of several polymers (gellan gum, hypromellose, xanthan gum, Carbopol) into the outer phase. The authors observed that hypromellose acts as a viscosity

enhancing agent that can prolong the intraocular pressure-lowering effect in glaucoma in rabbits[46].

J. Shen et al. developed a thiolated mucoadhesive polymer coated NLC in which cysteine-polyethylene glycol stearate conjugates were incorporated into the NLC formulation. Cyclosporine encapsulated in NLC was found to remain on the ocular surface for up to 6 h, resulting in an increased concentration in the anterior segment compared to NLC without thiomers[50]. Liu et al. studied several thiolated chitosan-modified NLC systems. The N-acetyl-L-cysteine-functionalized chitosan copolymer was synthesized and the modified polymer-coated NLC systems were compared with simple chitosan-coated NLCs. Modification of chitosan significantly improved transcorneal penetration compared to plain chitosan hydrochloride-coated and uncoated NLC[51].

Chanburee et al. investigated the effect of different polymers on the mucoadhesive properties of each NLC system. Curlin-containing NLCs were prepared in which the surface of the particles was coated with various mucoadhesive polymers such as polyethylene glycol 400 (PEG 400), polyvinyl alcohol (PVA) and chitosan (CS). Mucoadhesiveness was assessed by an in vitro wash away assay, and both PEG-NLC and PVA-NLC showed strong interactions with porcine mucosa and even more than twice as strong mucosal adhesion was observed than that of uncoated NLCs[52].

3. EXPERIMENTAL AIMS

In my PhD work, the aim was to increase the bioavailability of topically applied ophthalmic preparations, which I did along two main directions.

In the first part of my PhD work, I aimed to combine the good adhesion properties of the mucoadhesive polymers (thiolated poly(aspartic acid)) with increased solubility of corticosteroids using cyclodextrins, thereby increasing the bioavailability of the active ingredient.

The possible advantages of using a modified polymer can be the *in situ* gellable and strong mucoadhesive behavior derived from the basic polymer properties and the increased solubility of PR thanks to the grafted CD. In this case, the covalently bonded drug-cyclodextrin complex may not diffuse and wash out with the lacrimal drainage from the adherent layer of the ocular gel. Therefore the residence time of the formulation is increased, and an improved bioavailability of the lipophilic ocular drug, prednisolone can be provided.

The basic goal in the formulation of *in situ* gelling ophthalmic gels was to develop a well-tolerated, easy-to-use, and sustained-release formulation. In order to investigate biocompatibility, I used physiological and optical conformity studies (pH, osmolality,

transmittance and refractive index test) and rheological methods to assess *in situ* gelation after the application. Franz diffusion cells were used to study prolonged drug release *in vitro* (Fig. 4).

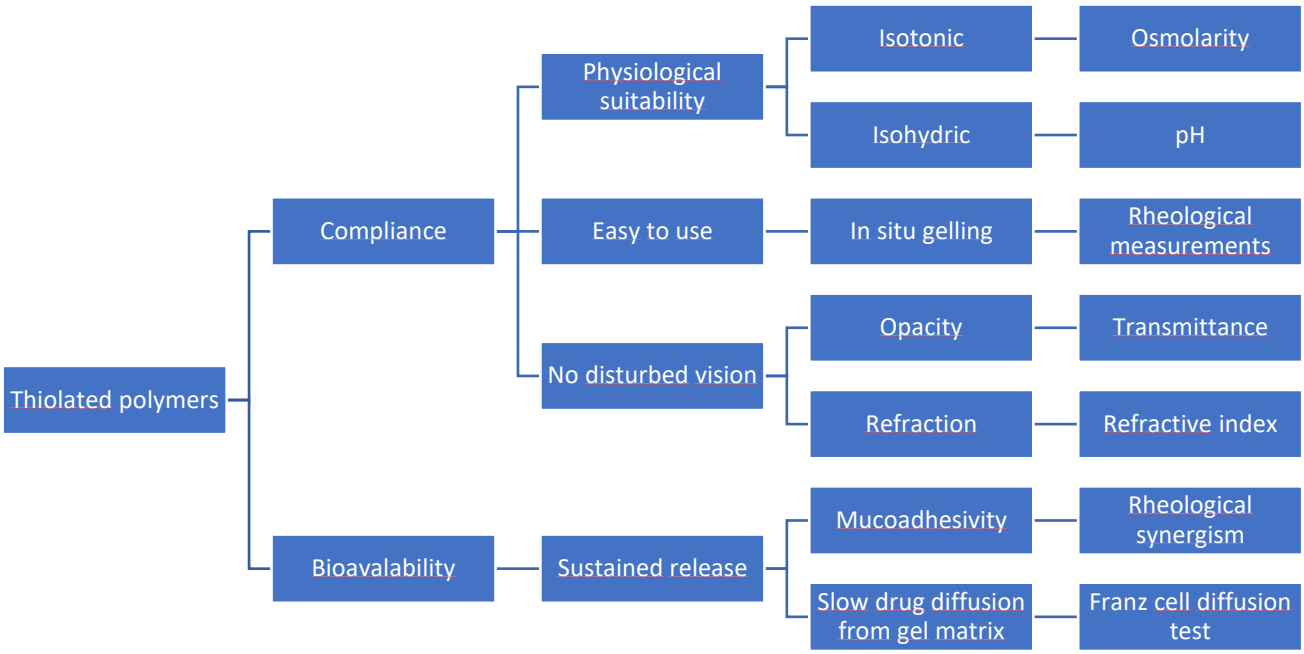

Figure 4*. Flow curve of the investigation of thiolated polymers*

The second part of my Ph.D. work can be divided into two main parts. In the first part, the aim was to improve the bioavailability of DXM by dissolving it in lipids and incorporate it into NLCs.

In the second part, the aim was to increase the ocular residence time of our formulations using a mucoadhesive polymer. Polymers have amphiphilic characteristics, which may result in their enrichment at the interface of the nanocarrier. Thus, a mucoadhesive gel layer can form around the nanoparticles. This way, the gel layer around the nanocarrier can ensure nanoparticle adhesion to the mucosal surface.

In the first part, as a preformulation study, lipid screening (visual observation, particle size, Span value determination) and crystallinity index measurements were performed. The state of the API in lipid matrix was determined by X-ray diffraction analysis. To characterize the nanostructured lipid carriers a 2^3 factorial experimental design was used. The optimization parameters were particle size, Zeta potential, polydispersity index, and entrapment efficiency. The ophthalmic applicability of NLC systems was verified by determination of mucoadhesivity, drug release study, and penetration study. The penetration of the DXM was examined with three different models: Corneal-PAMPA, HCE-T cells, and *ex vivo* Raman mapping. After the examination, the results of the drug release study and the

results of penetration studies (Corneal-PAMPA, HCE-T cells) were compared. The biocompatibility of NLC components and formulations were investigated with an immunohistochemistry method and a cell viability assay (Fig. 5.).

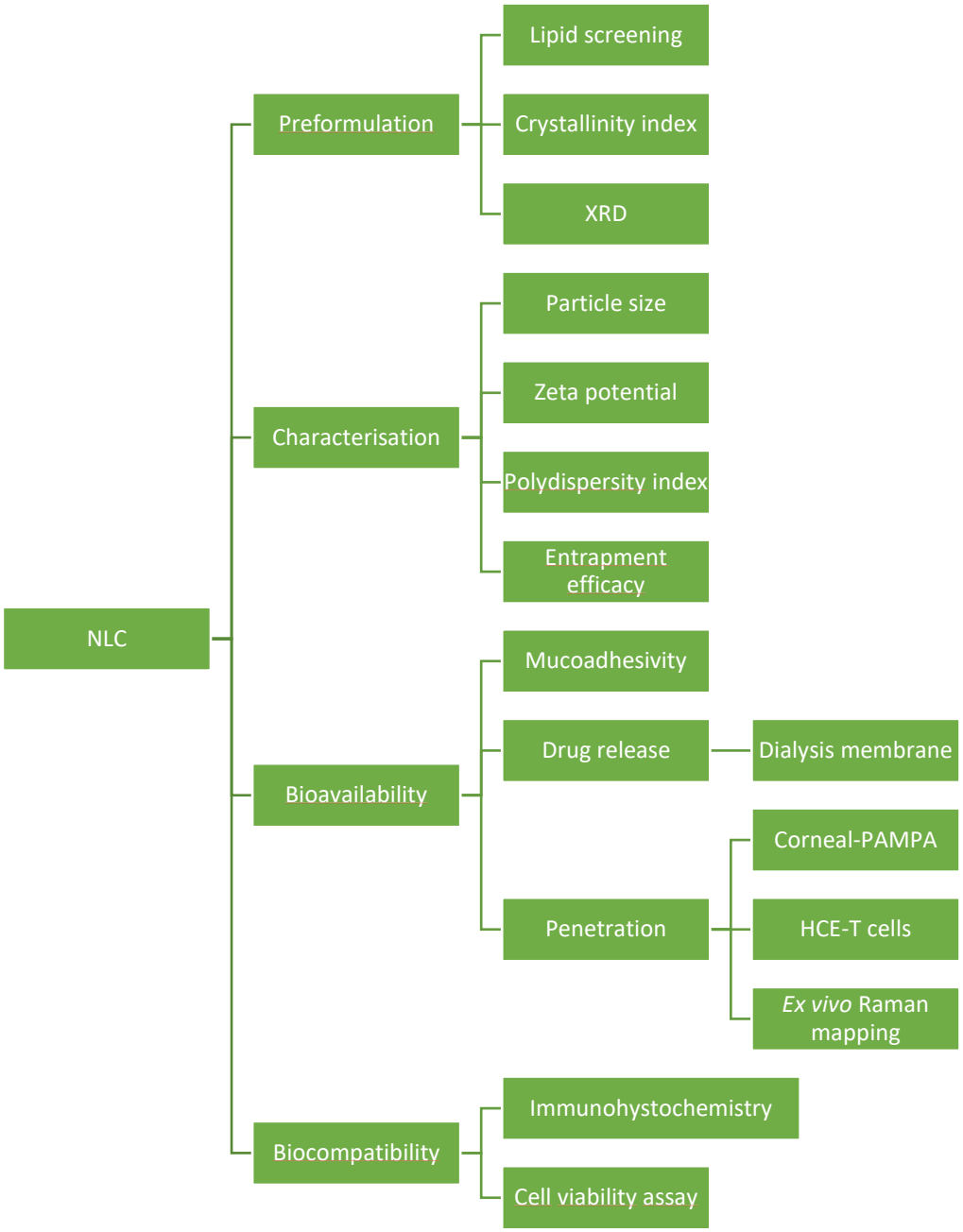

Figure 5*. Flow curve of the investigation of NLCs*

4. MATERIALS AND METHODS

4.1 Materials

4.1.1. Materials of in situ gelling systems

L-aspartic acid (puriss. 99.5%) was purchased from Merck, crystalline phosphoric acid (99%) was bought from Sigma-Aldrich. Cysteamine (95%), dibutylamine (a.r.), dithiothreitol (99%), *N*,*N*-dimethylformamide (a.r.) and sodium bromate (99%) were

purchased from Reanal Hungary. 6-monodeoxy-6-monoamino-beta-cyclodextrin hydrochloride (MABCD) was obtained as a gift from CycloLab Cyclodextrin Research and Development Laboratory Ltd. In the gel formulation, phosphate-buffered saline (PBS) solution of pH = 7.4 was prepared by dissolving 8 g dm^{-3} NaCl, 0.2 g dm^{-3} KCl, 1.44 g dm^{-3} $Na_2HPO_4*2H_2O$ and 0.12 g dm^{-3} KH_2PO_4 in distilled water, the pH being adjusted with 0.1 M HCl. In the mucoadhesive measurements, mucin (porcine gastric mucin type II) was purchased from Sigma-Aldrich, mucin dispersions were prepared with PBS, stirred for 1 h and left for overnight in a refrigerator.

4.*1.1.1. Thiolated polymers*

Thiolated polymers are second generation mucoadhesive polymers with thiol-containing side-groups, which are able to form disulphide bonds with cysteine-rich subdomains of the mucus layer, thereby providing strong adhesion to the mucosal surface. We had already displayed a new type of thiomers as a potential ocular excipient, where the thiol-containing side-groups were bonded to poly(aspartic acid), which is a biocompatible and biodegradable polymer thanks to its protein-like structure. The synthesized thiolated poly(aspartic acid) contains thiol side groups and in the presence of oxidizing agent, PASP-CEA is reversible cross-linked via disulphide bonds. The thiolated poly(aspartic acid) polymers were synthesized by Budapest University of Technology and Economics, Soft Matters Group as it was described by Budai-Szűcs et al.[53].

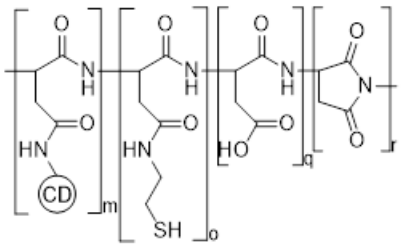

Figure 6*. Cyclodextrin-bonded thiolated poly(aspartic acid)*

In the case of the MABCD-PR complex, 10 mg PR was added to 1 mL of purified water containing different concentrations of MABCD (0–2.5% w/v). In the case of the PASP-CEA-CD–PR complex, 5 mg PR was added to 1 mL of purified water containing different concentrations of PASP-CEA-CD (0–10 % w/v) (Fig.6.). A solubility study was carried out[53]. The results suggested that the complexation ability of MABCD was changed only slightly by chemical immobilization onto the polymer based on the value of the stability constants (MABCD: 679 M^{-1} and PASP-CEA-CD: 506 M^{-1}).

4.1.1.2. Active pharmaceutical ingredients

In the thiolated hydrogel systems the applied active agent was prednisolone, which was obtained as a gift from TEVA Hungary Ltd. NLC formulations made with DXM which was kindly provided by Sigma-Aldrich (Germany). Prednisolone is a lipophilic and poorly water-soluble drug, thus its penetration through the cornea and its bioavailability are very poor.

Dexamethasone is a lipophilic drug with low water solubility. It has been used as a suspension type eye drop with a dose of 0.05% and 0.1%.

These corticosteroids are often used in the treatment of various ophthalmic inflammatory diseases[54]. However, its poor penetration through the cornea results in poor bioavailability. On the other hand, DXM can be dissolved in certain lipids.

4.1.2. Materials of NLC systems

Compritol 888ATO (glycerol dibehenate; melting point: 65 – 77 °C), Apifil (PEG-8 beeswax, HLB value: 9) Labrasol (Caprylocaproyl Polyoxyl-8 glycerides, HLB value: 12) were kindly supplied by Azelis Hungary Ltd (Hungary). Miglyol 812N (capric triglyceride) were provided by Sasol GmbH (Germany). Kolliphor EL (Polyoxyl 35 hydrogenated castor oil, HLB value: 12-14) and Cremophor RH60 (PEG-60 hydrogenated castor oil, HLB value: 15-17) were kindly supplied by BASF SE Chemtrade GmbH (Hungary). Tween 20 (Polysorbate 20, HLB=16,7) were purchased from Hungaropharma Ltd (Hungary). Hydroxypropyl methylcellulose (Methocel F4M) was purchased from Colorcon (Dartford, Kent, England).

The applied API was dexamethasone, mentioned in section 4.1.1.2.

4.2. Methods of investigation of thiolated polymers

4.2.1. Preformulation study

As preformulation study the osmolality, refractive index and pH were measured in aqueous solutions of PASP-CEA and PASP-CEA-CD at 10% w/v[53]. The osmolality of the polymer solutions was measured by means of an automatic osmometer (Knauer Semi-micro Osmometer, Berlin, Germany) in three parallels. The determination of osmolality is based on the measurement of the freezing point depression of the solution. The pH of the polymer solutions was measured with a pH-meter (Testo 206-pH2, Hampshire, UK)

4.2.2. X-ray diffraction study of cyclodextrin-prednisolone complexes

The inclusion complexes were characterized by an X-ray powder diffractometer (XRPD) (D8 Advance diffractometer, Bruker AXS GmbH, Billerica, MA, USA) using Cu K λI radiation (λ =1.5406 Å). Each sample was scanned at 40 kV and 40 mA in the interval 3–

40° 2θ (at 0.1/second scanning speed and with 0.010° step size). PR, PASP-CEA-CD powder and the lyophilized (ScanVac CoolSafe lyophilizer, Labogene, Allerod, Denmark) supernatant of the solution of MABCD-PR (2.5% w/v MABCD, 0.4 % w/v PR) and PASP-CEA-CD–PR (10.2% w/v PASP-CEA-CD, 0.15% w/v PR) prepared for the solubility study were investigated by XRPD. After sample preparation, the formulations were freeze-dried.

4.2.3. Rheological measurements

The rheological measurements were carried out with a Physica MCR101 rheometer (Anton Paar, Graz, Austria). The measuring device was a parallel plate type (diameter 25 mm, gap height 0.100 mm). Gelation was followed by oscillatory rheological tests and gels were also characterized by rheometry. The oxidizing circumstance in the eye was simulated with sodium bromate [13]. In the gelation measurements, the polymer solutions (the final concentration was 10% w/w) were mixed with 1 M oxidant (the final concentration of the oxidant solution was 20% w/w) on the plate of the rheometer and the measurement was started immediately. The gelation was followed at a constant angular frequency of 1.0 s^{-1} at a constant strain of 1% at 25 °C. The viscoelastic properties of the formed gels were determined by frequency sweep tests after total gelation, with a strain of 1%, over the angular frequency range from 0.1 to 100 s^{-1} at 25 °C.

To study mucoadhesion, the polymer solutions were mixed with the mucin dispersion (the final mucin concentration was 5% w/w) in PBS before the addition of the oxidant. The rheological synergism was calculated.

4.2.4. Drug release study

The drug diffusion profile of PR was determined with a vertical Franz diffusion cell system (Hanson Microette Plus TM)[53]. The donor phase was a formulation containing 10% w/w polymer (PASP-CEA or PASP-CEA-CD), 0.1% w/w PR and 20% w/w oxidant solution. The gelation occurred *in situ* after the installation. The diffusion membrane was a Porafilm membrane (pore size of 0.45 μm). The acceptor phase was PBS (pH = 7.4) and it was thermostated at 35 °C. The PR released was measured at 247 nm by a UV-VIS spectrophotometer (Thermo Scientific Evolution 201).

4.3. Methods of investigation of NLC systems

4.3.1. Preparation of NLC systems

For the preparation of the NLC samples (Table 1.), an ultrasonication method was used[55,56]. The lipids (Compritol 888 ATO and Miglyol 812N at 7:3 ratio) and surfactant (Kolliphor RH40) were melted with a heating magnetic stirrer at 85 °C. After that, DXM and the polymer (hypromellose: Methocel F4M) were added to the melted mixture and stirred at

of 85 °C. Pure water was heated to 85 °C and the two phases were mixed, ultrasonicated and then cooled in an ice bath.

Table 1. *The composition of NLC systems.*

		Lipid concentration (w/w%)	DXM concentration (w/w%)	Surfactant concentration (w/w%)	Polymer concentration (w/w%)
Basic NLC formulation (Factorial design 1)	NLC1	10	0.05	2.5	-
	NLC2	15	0.05	2.5	-
	NLC3	10	0.10	2.5	-
	NLC4	15	0.10	2.5	-
	NLC5	10	0.05	5.0	-
	NLC6	15	0.05	5.0	-
	NLC7	10	0.10	5.0	-
	NLC8	15	0.10	5.0	-
Mucoadhesive NLC formulation (Factorial design 2)	NLC9	10	0.05	2.5	0.05
	NLC10	10	0.05	2.5	0.10
	NLC11	10	0.05	5.0	0.05
	NLC12	10	0.05	5.0	0.10
	NLC13	10	0.10	2.5	0.05
	NLC14	10	0.10	2.5	0.10
	NLC15	10	0.10	5.0	0.05
	NLC16	10	0.10	5.0	0.10

4.3.2. X-ray diffraction of lipid compositions

The solid state of DXM in the lyophilized lipid composition and the freeze-dried NLC formulations was analyzed with XRD. The XRD measurements were performed with a Bruker D8 Advance diffractometer (Bruker AXS GmbH, Karlsruhe, Germany). The method was described in section 4.3.2.

4.3.3. Investigation of lipid crystallinity with DSC measurements

The crystallinity index of lipid mixtures and DXM containing lipid mixtures were examined with DSC (Mettler-Toledo 821e DSC instrument (Mettler-ToledoGmbH, Greifensee, Switzerland))[55]. The sample compositions are listed in Table 2.

Table 2. *The composition of lipid mixtures (LMs) for XRD and DSC measurements in w/w%.*

	Compritol 888 ATO	Miglyol 812N	Kolliphor EL	Cremophor RH60	DXM
LM-1	70.00	30.00	-	-	-
LM-2	90.00	10.00	-	-	-
LM-3	46.67	20.00	-	33.33	-
LM-4	46.67	20.00	33.33	-	-

LM-5	60.00	6.67	33.33	-	-
LM-6	60.00	6.67	-	33.33	-
LM-7	46.67	20.00	-	33.33	0.33
LM-8	46.67	20.00	33.33	-	0.33
LM-9	60.00	6.67	33.33	-	0.33
LM-10	60.00	6.67	-	33.33	0.33

4.3.4. Particle size and zeta potential of NLCs

The hydrodynamic diameter (Z_{ave}), zeta potential (ZP), and polydispersity index (PI) of NLCs were investigated by a Zetasizer Nano ZS instrument (Malvern Instruments, Worcestershire, UK) with a DTS 1070 folded capillary cell at 25 °C.

Laser diffraction was used to analyze The NLCs (Table 1.) the particle size and particle size distribution of NLCs (Table 1.). Laser diffraction measurements were carried out using a Mastersizer 2000 Hydro tool (Malvern Instruments, Worcestershire UK). The d(0.1), d(0.5) and d(0.9) values were assessed.

In order to evaluate the stability of NLCs, the particle size and ZP measurements were repeated during storage.

4.3.5. Entrapment efficiency of NLCs

The entrapment efficiency (EE%) of NLCs was determined with an indirect method. The clear aqueous phase of the NLCs was separated by centrifugation in Vivaspin 15R 5,000 MWCO Hydrosart tubes (Sartorius, Stonehouse, UK) with Hermle Z323K, (HERMLE Labortechnik GmbH, Wehingen, Germany)[55,56].

The DXM content of the filtered solution was examined by HPLC (Shimadzu Nexera X2 UHPLC, Kyoto, Japan), which was equipped with a C18 reverse-phase column (Phenomenex Kinetex EVO C18, Phenomenex, Torrance, CA, USA) with dimensions of 1.7 µm, 100 Å, 100 * 2.1 mm. The mobile phase was water:acetonitrile 75:25 in isocratic elution, the detection was made at 240 nm. The injection volume was 5 µl and the flow rate was 0.5 mL/min.

The following equation was used to calculate EE% :

$$EE\ \% = \frac{W_{initial\ drug} - W_{free\ drug}}{W_{initial\ drug}} \times 100 \quad (1)$$

where the $W_{initial\ drug}$ weight of the initial drug and the $W_{free\ drug}$ was the weight of the free drug, which was solved in the outer phase.

4.3.6. In vitro drug release study

Considering the results of the factorial experimental design, four NLC compositions were selected for diffusion study[55]. To investigate *in vitro* drug release, a dialysis bag method was used. Firstly, 200 µL of the samples were put in a Spectra/Por® 4 dialysis membrane (Spectrum Laboratories, Inc., Rancho Dominguez, CA, USA) and sealed with Spectra/Por® Closures (Spectrum Laboratories, Inc.). The acceptor phase was 20 mL of phosphate-buffered saline (PBS). As reference preparation, a DXM suspension was applied. The diffused amounts of DXM were analyzed by HPLC (the HPLC method is described in Section 4.4.4)

4.3.7. Human HCE-T corneal epithelial cell line

Human corneal epithelial cells (HCE-T; RCB 2280; RIKEN BRC, Tsukuba, Japan) were immortalised by transfection with a recombinant SV40-adenovirus vector, established and characterized by Araki-Sasaki[57]. The method was described by Kiss et al.[55,56].

4.3.8. Cell viability measurements

Real-time cell electronic sensing was used to follow cell damage and/or protection in living barrier forming cells[55,56].

The investigated samples were Cremophor RH60 and DXM NLC3, NLC7, NLC9, NLC10, NLC11, NLC12 formulations and hypromellose solution.

4.3.9. Immunohistochemistry

Morphological changes in HCE-T cells were investigated by immunostaining for junctional proteins, zonula occludens protein-1, occludin, β-catenin, and E-cadherin. Cells were grown on culture inserts used for permeability experiments[56].

4.3.10. Experimental design

In order to characterize the polymer containing NLC compositions, a 2^3 full factorial design was applied, which is suitable for generating a first-order polynomial model (eq. 2) and for the investigation of the linear response surface. The model describes the principal effects and interaction among the identified variables.

$$y = a_0 + a_1x_1 + a_2x_2 + a_3x_3 + a_{12}x_1x_2 + a_{23}x_2x_3 + a_{13}x_1x_3 \qquad (2)$$

where a_0 is the intercept, $a_{1,2,3}$ were the regression coefficients values. x_1, x_2, and x_3 correspond to factors A, B and C, respectively.

In the first factorial experimental design the independent factors were A (lipid concentration), B (DXM concentration) and C (surfactant concentration). In the second case the independent factors were A (polymer concentration), B (DXM concentration) and C (surfactant concentration).

The optimization parameters were indicated in each measurement, when they were applicable. The chosen factors were examined at two levels (+1 and -1), which corresponds to the values in Table 1.

4.3.11. Mucoadhesion study

The mucoadhesion of polymer containing and polymer free formulations were investigated with a TA.XT plus Texture Analyzer (Stable Micro Systems Ltd., Vienna Court, Lammas Road, Godalming, Surrey, UK. GU7 1YL). A cylinder probe with a diameter of 1 cm[58,59]. Samples were placed in contact with a filter paper disc wetted with 50 μL 8% w/w mucin dispersion as *in vitro* mucosal surface[59]. 20 mg of the sample was attached to the fixed filter paper of the cylinder probe and placed in contact with the artificial mucosal surface. After the preload, the cylinder probe was moved upwards to separate the sample from the substrate. The work of adhesion (A, mN mm) was used to characterize the mucoadhesive behavior.

4.3.12. Penetration study on corneal-PAMPA model

For the *in vitro* transcorneal permeability measurement, a corneal-PAMPA method was applied[60]. DXM and its formulations were used as a donor solution. In order to create the lipid membrane, phosphatidylcoline (PC, 16 mg) was dissolved in a solvent mixture (70% v/v hexane, 25% v/v dodecane, 5% v/v chloroform), and then each well of the donor plate (MultiscreenTM-IP, MAIPN4510, pore size 0.45 mm; Millipore) was coated with the lipid solution (5 μL each). Then hexane and chloroform were evaporated to form a PC lipid membrane. The donor plate was fit into the acceptor plate (Multiscreen Acceptor Plate, MSSACCEPTOR; Millipore) containing 300 μL of PBS solution (pH 7.4), and 150 μL of the PBS solutions were put on each membrane of the donor plate. The plates were incubated for 4 h at 35 °C (Heidolph Titramax 1000) then PAMPA sandwich plates were separated. API concentrations in the donor and acceptor solutions were determined by HPLC method (the HPLC method is described in Section 4.4.4.). The effective permeability and membrane retention of drugs were calculated using the following equation (eq. 3)[60]:

$$P_e = -\frac{2.303 \cdot V_A}{A(t-\tau_{SS})} \cdot \log\left[1 - \frac{c_A(t)}{S}\right] \quad (3)$$

where P_e is the effective permeability coefficient (cm s^{-1}), A is the filter area (0.24 cm^2), VA is the volume of the acceptor phase (0.3 cm^3), t is the incubation time (s), τ_{SS} is the time to reach steady-state (s), $C_A(t)$ is the concentration of the compound in the acceptor phase at time point t (mol cm^{-3}), S is the free drug content of DXM in the donor phase.

4.3.13. Permeability study on cell culture model

Transepithelial electrical resistance (TEER) was measured to check the barrier integrity by an EVOM volt-ohmmeter (World Precision Instruments, Sarasota, FL, USA) combined with STX-2 electrodes. TEER was expressed relative to the surface area of the monolayers as $\Omega \times cm^2$. TEER of cell-free inserts was subtracted from the measured data. Cells were treated when the cell layer had reached steady TEER values[56].

For the permeability experiments the inserts were transferred to 12-well plates containing 1.5 mL Ringer buffer in the acceptor (lower/basal) compartments. In the donor (upper/apical) compartments 0.5 mL buffer was pipetted containing different formulations of DXM (10-times dilution of NLCs). Samples from both compartments were collected and the DXM concentration was detected by HPLC.

The apparent permeability coefficients (P_{app}) were calculated as described by Bocsik et al.[61]. Briefly, cleared volume was calculated from the concentration difference of the tracer in the acceptor compartment ($\Delta[C]_A$) after 30 minutes (Δt) and donor compartments at 0 hour ($[C]^D$), the volume of the acceptor compartment (V_A; 1.5 mL) and the surface area available for permeability (A; 1.1 cm^2) using this equation (eq. 4):

$$P_{app}\ (cm/s) = \frac{\Delta[C]_A \times V_A}{A \times [C]^D \times \Delta t} \qquad (4)$$

For permeability measurements NLC5, NLC6, NLC7, NLC8 formulations were applied at 10 times dilution and DXM at 1 mg/mL concentration, all diluted in Ringer-Hepes buffer.

4.3.14. Penetration study on porcine cornea

The *ex vivo* penetration test was examined with Raman microscopy. The pig conjunctiva came from a slaughterhouse and was kept at -20 °C until measurement. The cornea was instilled with 250 µL of NLC sample (NLC14 and the polymer-free version of NLC14) every 30 min and the formulation was removed just before the next instillation[55,56]. The duration of treatment was six hours. The treated cornea was frozen and divided into cross sections (20 µm thick) onto aluminum-coated slides using a Leica CM1950 cryostat (Leica Biosystems GmbH, Wetzlar, Germany). Untreated porcine cornea was used as a reference. Raman microscopic measurements were performed with a Thermo Scientific DXR Raman microscope (Thermo Fisher Scientifc, Waltham, MA, USA). We used 780 nm laser light with a maximum power of 24 mW. The setting parameters was described by Kiss et al.[55,56]. During the evaluation, profiling of the Raman map was performed using the entire NLC spectrum.

4.3.15. Statistical analysis

The release test results were analyzed statistically with two-way ANOVA analysis with Bonferroni post-tests.

For the MTT and cell penetration assays, the values were compared using ANOVA followed by Dunett's test or 2-way ANOVA followed by the Bonferroni post-test. The values are expressed as means ± standard deviation (SD). A level of $p \leq 0.05$ was taken as significant (*), $p \leq 0.01$ as very significant (**), and $p \leq 0.001$ as highly significant (***).

The factorial experimental designs were evaluated with Statistica for Windows, version 10.

5. RESULTS

5.1. Investigation of thiolated polymers

5.1.1. Preformulation study

5.1.1.1. Formation of inclusion complexes

The inclusion of PR within MABCD and PASP-CEA-CD was investigated by XRPD. Diffractograms of PR, MABCD, PASP-CEA-CD, MABCD-PR and PASP-CEA-CD-PR were recorded (Fig. 7.).

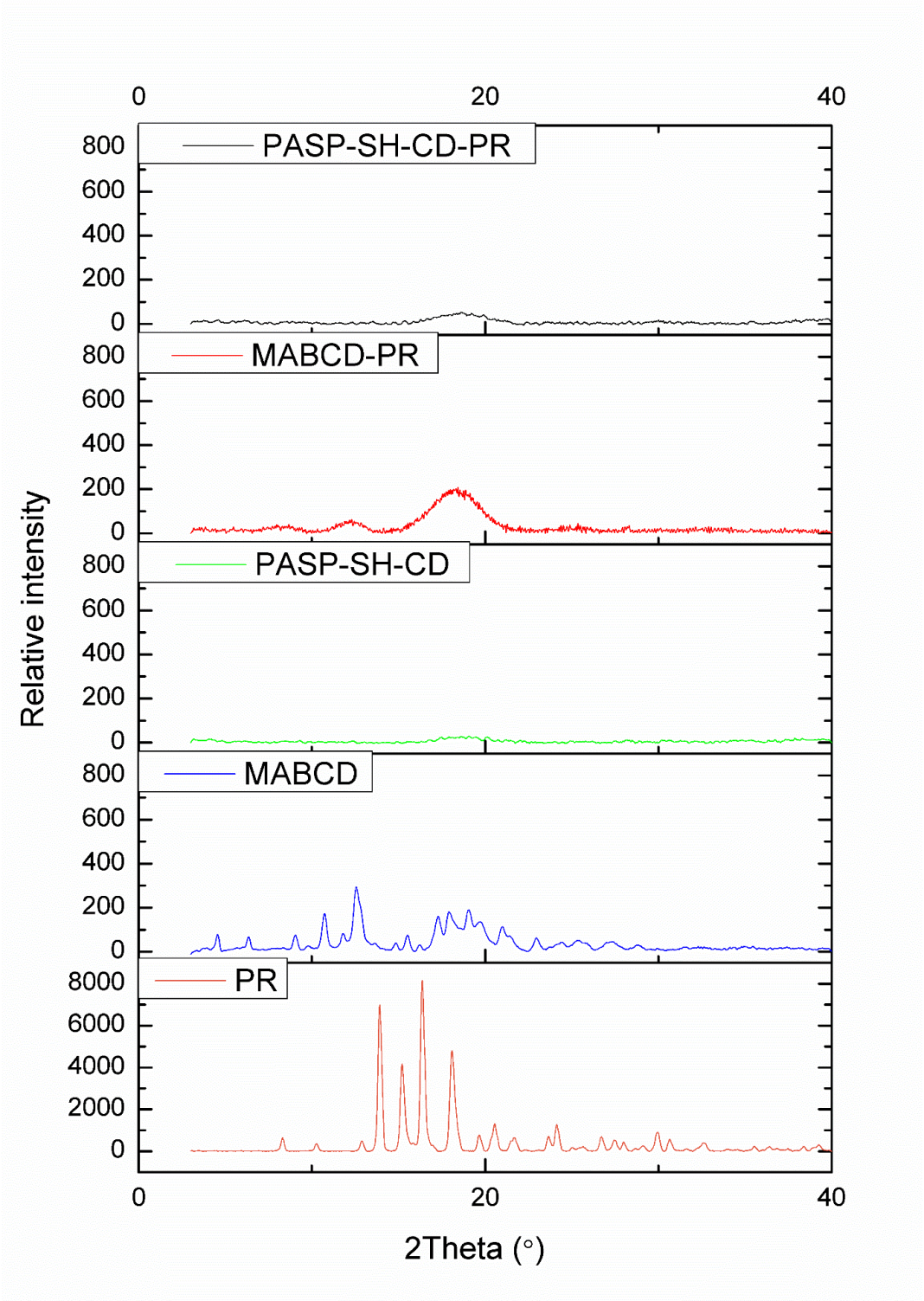

Figure 7*. X-ray powder diffractogram of PR, MABCD, PASP-CEA-CD, and complexes of PR with MABCD and PASP-CEA-CD.*

The diffractogram of PR showed a crystalline structure, indicated by the sharp peaks in the graph. In the case of the polymer (PASP-CEA-CD) and the cyclodextrin (MABCD), an amorphous pattern can be observed, there is no high intensive characteristic peak in the diffractogram. In the case of inclusion complexes, no characteristic peak of PR can be seen

in the pattern, the amorphous structure of PASP-CEA-CD and/or MABCD dominates. The absence of the crystalline peaks of PR can prove the formation of the inclusion complexes.

5.1.1.2. Measurement of osmolality, pH and refractive index

Several excipients that are applied in ocular drug formulations can alter the physical and physiological properties and the stability of the tear film[62–64]. In one of our studies, we investigated the physiological acceptability of PASP-CEA polymers[65]. We established that PASP-CEA is a promising eye drop excipient as the PASP-CEA solution had similar physicochemical characteristics to those of tear fluid or it did not affect them[59,65]. We modified the polymer by grafting MABCD to the polymer backbone. The physiological characteristics of the PASP-CEA and PASP-CEA-CD solution were measured and compared with each other and the tear fluid.

The osmolality of the tear film in a normal eye is 300 to 310 $mOsmL^{-1}$. In our case, the osmolality of neither polymer solution was measurable at the applied concentration with this methodology, which indicates the possibility and the necessity of the addition of excipients, such as an isotonizing agent. In some cases, the hypoosmolality of the ophthalmic solution is required, especially in artificial tears in the treatment of dry eye disease[66].

The refractive indexes of the polymer solutions (PASP-CEA: 1.3494; PASP-CEA-CD: 1.3478) were very close to that of the tear film (1.3370), which suggests the formulation does not disturb the vision of the patient.

The pH range of 6 to 9 is tolerable for the eye. In this range, the formulation does not cause discomfort. Outside this range, increased lacrimation can be expected due to irritation[67]. The pH of both solutions prepared with distilled water was lower than physiological (pH = 4.7 of PASP-CEA and 5.0 of PASP-CEA-CD solutions), but when pH = 7.4 PBS solution was the solvent, the pH remained 7.4, indicating the low buffering effect of the polymers.

5.1.2. Gelation and mucoadhesivity

The PASP-CEA solution exhibited *in situ* gelling via disulphide linkages. The gelation is affected by environmental factors, such as the oxidant and polymer concentration[59] and polymer structural factors, the thiol content of the polymer[68] and the type of the side groups[65]. The polymer was modified with MABCD. The gelation process, the gel structure and the mucoadhesion of the modified polymer were characterized by means of rheology.

Gelation time is a critical factor in the case of an *in situ* gelling ophthalmic formulation: too fast gelation results in inadequate spreading on the ocular surface, therefore

foreign body sensation is caused to the patient, while prolonged gelation leads to too fast elimination due to blinking and lacrimation[69]. Different polymer solutions were investigated in order to clarify the effect of the CD side group or several additives without grafting, such as MABCD, PR. The PASP-CEA solution displayed a fast solution-to-gel transition in the presence of an oxidant, gelation occurs within 200 seconds in all formulations (Fig 8).

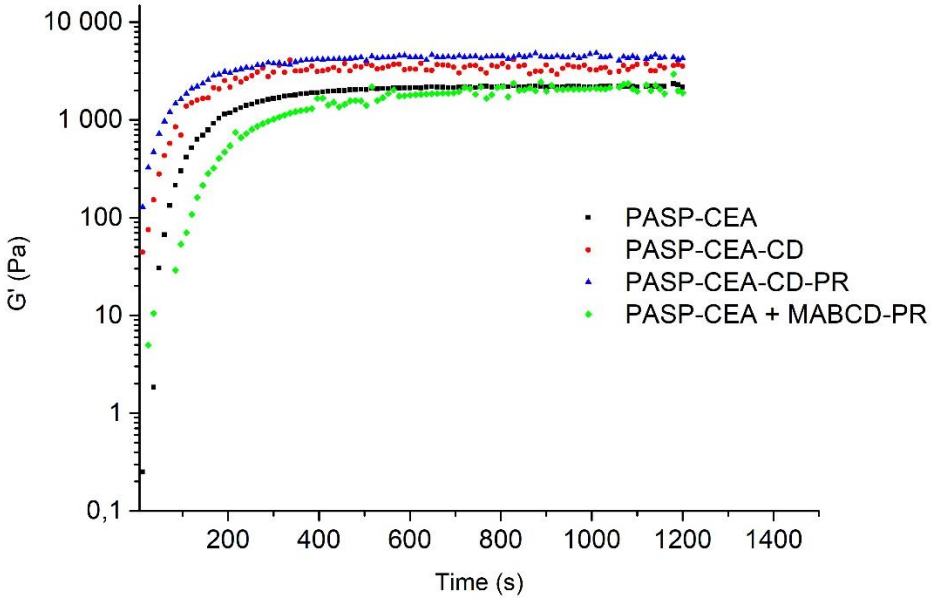

Figure 8. *Gelation of the different polymer solutions.*

Fig. 8 demonstrates that the immobilization of MABCD on the polymers did not hinder the gelation process and similar gelation times were observed for polymers containing PR in the complex. The structures developed during gelation were also similar for each sample proven by the frequency sweep tests (Fig. 9), which showed final G' values in the range of a few kPa independently of the chemical composition and also the presence of drug molecules. The moduli were constant over the whole frequency range, indicating a coherent chemical gel structure in all cases.

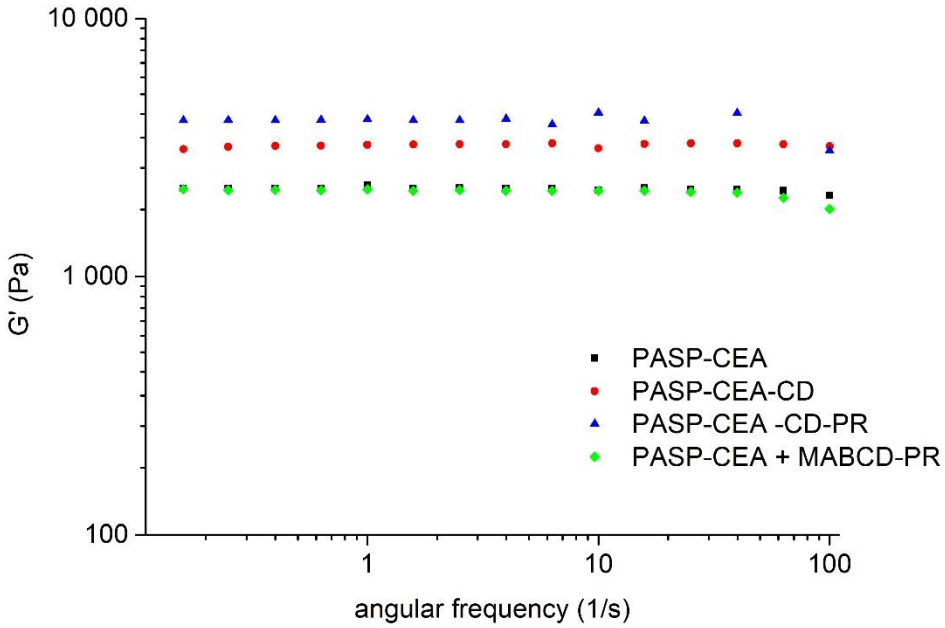

***Figure 9**. Frequency sweep test of the gel formulations.*

Mucoadhesion was characterized by means of the synergism parameter calculated from the G' values at 1.0 1/s angular frequency[70].

In our calculation the synergism parameters of the PASP-CEA and PASP-CEA-CD were 1370 and 1390 Pa, respectively. The similar data mean similar mucoadhesivity, thus as a conclusion, the modification of the polymer with MABCD did not change the mucoadhesive characteristics of the PASP-CEA polymers.

5.1.3. Drug release study

The complexation of PR with CDs improves PR solubility in aqueous medium. The complexes diffuse in the formulation and can carry the PR molecules through the aqueous mucin layer[71]. Due to the free diffusion of the complex inside the formulation, the active compound can be washed out with the drainage of the eye, even if a prolonged residence time of the formulation is provided by mucoadhesion. In my PhD work, CD is covalently attached to PASP-CEA, which hinders the diffusion of the complex, thus increasing the residence time of the formulation and the active agent on the ocular surface. In this case, slower and prolonged drug release is expected because the drug molecules must be dissociated from the cyclodextrin molecules and diffuse through the aqueous tear fluid before reaching the absorption barrier. Since secondary interactions between PR and cyclodextrin units are formed and broken in a reversible manner, the affinity of PR to the CD's cavity will influence the rate of the drug release. On the other hand, it must be taken into consideration that the lipophilic drug may also be replaced by some other lipophilic molecule from the ocular surface (e.g. lipids from the tear film) if it has higher affinity to the central cavity of CD, and it can also have an effect on the drug release rate.

In my work, the release profile from the grafted and the free CD systems were compared *in vitro* (Fig. 10). The release profile of PASP-CEA gel formulation containing free MABCD-PR was very similar to that of PR suspension (no significant differences, $p > 0.05$), which can be the result of two effects. The solubility of the active compound is higher, which would improve the release, but the rate of drug release is limited by the presence of the polymer gel. The difference between the bioavailability of the simple suspension and the bioadhesive formulation derives from the different residence time. In this *in vitro* release test, the elimination mechanisms are not included, thus the differences in the release profile could not be observed. When MABCD was covalently attached to PASP-CEA, the diffusion of the complex was blocked, only free PR was able to diffuse through the membrane, thus the release rate was slower and depended on the PR dissociation from the CD molecule. Very significant differences could be observed ($p \leq 0.01$) between the drug release from the basic and CD grafted polymer gel after two hours and highly significant ($p \leq 0.001$) differences after three hours. The drug release profile of the PASP-CEA-CD-PR complex can be divided into three sections: in the first two hours, the significant concentration gradient between the donor and the acceptor phase resulted in a fast release; after that an intermediate section can be observed between the 2^{nd} and 6^{th} hours, while from the 6^{th} hour a slow continuous drug release can be seen, which can be described with zero order kinetics. The recovery of the eye surface typically occurs within 24 hours, thus during the formulation of mucoadhesive ocular drug delivery, a maximum duration of action of 24 hours can be designed. The PASP-CEA-CD-PR complex enabled the release of only 66% of the incorporated drug within 24 hours. Therefore, to accelerate the amount of released drug, 50% of MABCD was applied in free form, while the 10% w/w polymer concentration was ensured with the incorporation of 5% w/w PASP-CEA. In this case, an intermediate drug release profile between the grafted and free MABCD can be observed, which indicates that with the combination of the free and grafted MABCD, the drug release profile can be modified within the two limiting profiles. The combination can be beneficial because there are some free complexes which can diffuse faster to the corneal surface and provide a fast biological effect, while the bounded complex provides a slow, prolonged drug release for up to 24 h.

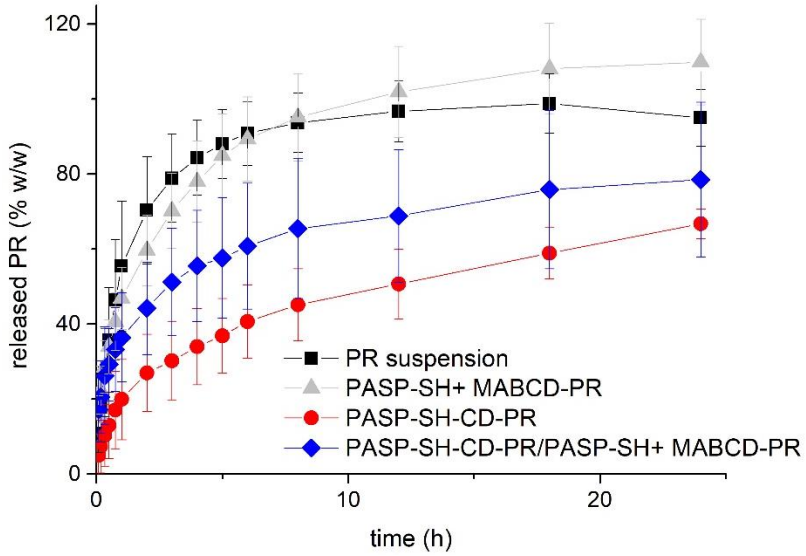

***Figure 10**. Drug release from the formulations containing PR.*

5.1.4. Conclusion

The aim of this work was to increase the solubility and residence time of prednisolone in a hydrophilic mucoadhesive ophthalmic formulation. Accordingly, increased residence time with mucoadhesive polymers and improved solubility with the application of CD were combined in the same in situ gelling formulation. The intended PR concentration in the form of a solution was 0.1% w/w. Two approaches were used: MABCD was dissolved in the mucoadhesive polymer solution, or CD was grafted onto the mucoadhesive polymer prior to gelation. Chemical binding of MABCD with PASP-CEA polymer did not alter the CD complex with PR, while the hydrogel retained its mucoadhesion. The drug release studies showed that grafting prolonged the drug release and achieved the best release profile with a combination of free and bonded CDs. The free complex can diffuse rapidly to the site of absorption, while the bounded complex allows for a long-term effect.

5.2. Investigation of dexamethasone loaded NLC formulations

5.2.1. Preformulation of NLC systems

5.2.1.1. Lipid screening

NLCs contain solid lipid, liquid lipid and surfactant in an aqueous medium. In my work, the selection criteria of the components were the low irritation potential, the eye tolerability and the suitability for NLC formulation based on literature background.

The lipid screening focused on 3 potential critical factors which may affect the performance of NLCs. The first was to find lipid compositions which are able to solve the applied dose of DXM. In the first part of the solubility study, a visual observation was used to detect insoluble DXM crystals in the different combinations of lipid melts. In the second part of this study, the solubility of DXM in the solidified lipids was analysed with XRD

measurements. The second critical factor can be the crystallinity of the applied lipids because their crystallinity index (CI%) may have an effect on the drug loading capacity of NLCs. This factor was investigated with DSC measurements. The third critical factor is the ability of the lipid-surfactant blends to form an NLC formulation, therefore blank (drug-free) test NLCs (T-NLCs) were formulated and analysed by laser diffraction.

5.2.1.2. Visual observations of DXM solubility

In this part of the solubility study, a fast screening method was applied, i.e. the visual observation of different combinations of lipid melts: solid lipids, liquid lipids alone and their mixtures with and without surfactant. When insoluble particles were observed in the thin layer of the melted lipid, it was considered as not dissolved.

Based on the results, there was no difference between the two solid lipids (Compritol 888 ATO and Apifil). The results of the comparison of Miglyol and Labrasol showed that Miglyol was much more effective at dissolving the API. In the case of solid lipid (Compritol 888 ATO), oils (Miglyol, Labrasol) and surfactant (Cremophor RH60, Kolliphor EL) containing mixtures, DXM was dissolved in almost all cases, where the mixtures were made with Apifil, Miglyol, Cremophor RH60, or Kolliphor EL.

5.2.1.3. XRD analysis of the lipid-API mixtures

The first section of the solubility study revealed that the lipid mixtures containing solid, liquid lipids and surfactant were able to solve the required DXM amounts. This section focused on the state (molecularly dispersed, amorphous or crystalline) of DXM in these solidified lipid mixtures with the aim of clarifying the effect of the solid lipid and liquid lipid ratio on the dissolution of DXM. To analyse the latter, 7:3 and 9:1 ratio of the solid and liquid lipids were evaluated.

The fact that the characteristic peaks of crystalline DXM are not detectable can prove that the API is amorphous or molecularly dispersed in all the lipid matrices and it can be concluded that the ratio of the solid and liquid lipids did not influence this behaviour.

On the other hand, the characteristic peaks of the solid lipids can be found in the lipid mixtures, indicating the presence of some crystalline solid lipid in all cases. The amount of crystalline solid lipid was detailed with DSC measurements in the next section.

5.2.1.4. Investigation of lipid crystallinity with DSC measurements

Lipid crystallization plays a very important role in the performance of NLC carriers because it has a great influence on the drug loading capacity of lipid particles and the drug release from them.

As it was mentioned, a strategy to decrease crystallinity is the application of liquid lipids, in my work two oil and solid lipid ratios (7:3 and 9:1) were evaluated. On the other hand, emulsifiers can also have an effect on crystallinity, so two emulsifier types (Cremophor RH60 and Kolliphor EL) in the same concentration were also investigated in this section.

The two emulsifiers (Cremophor RH60 and Kolliphor EL) reduced the crystallinity index, but there was no remarkable difference between them (Table 3.). The higher liquid lipid concentration resulted in the most relevant crystallinity index (CI%) depression. The presence of the API can also change the CI%, but just in the case of the 7:3 solid lipid-oil ratio. In this latter case, a slight increase in CI% could be observed [55].

Table 3. *The crystallinity index (%) of the lipid mixtures*[55].

Sample name	Crystallinity index (%)
LM-1	47.09
LM-2	82.90
LM-3	20.95
LM-4	18.33
LM-5	36.84
LM-6	36.26
LM-7	23.26
LM-8	23.11
LM-9	37.92
LM-10	34.02

Thanks to the favourable CI% depression effect of the 7:3 solid lipid-oil ratio (with minimal melting point depression), this ratio was applied for further optimization.

5.2.1.5. Selection of the potential NLC components

In order to clarify the ability of the chosen lipid mixtures to form a nanosystem, drug-free test NLCs were made. To characterize the NLC systems, the following factors were measured using the laser diffraction method: d(0.1), d(0.5), d(0.9) and Span values.

The lower Span value (at about 1 or less) indicates a more monodisperse distribution, thus better stability for NLC systems. On the basis of our results[55], Compritol 888 ATO, Miglyol 812N, Cremophor RH60 were chosen for further measurements and formulation optimization.

5.2.2. Optimization of DXM-loaded NLCs with factorial experimental design

5.2.2.1. NLC formulation

During the lipid screening, we could conclude that the optimal components for NLC formulation are Compritol 888 ATO, Miglyol 812N and Cremophor RH60 with a 7:3 solid lipid-liquid lipid ratio. To evaluate the effect of the component concentration and find the

optimal ratio, a factorial experimental design was used. With the application of a 2^3 full factorial design, over the optimal ratio, information about the interactions of factors can also be provided. Three formulation parameters of DXM-NLC were chosen as independent factors (the concentration of the emulsifier, the drug and the total lipid). As for the optimization parameters (dependent factors), the particle size (Z_{ave}), zeta potential (ZP), polydispersity index (PDI) and entrapment efficiency (EE%) of the NLC systems were chosen.

In the factorial design, the two levels of emulsifier concentration were 5% and 2.5%. As the high lipid concentration can make it possible to solve more API, 10 and 15% total lipid contents were evaluated with 0.05 and 0.1% total DXM concentrations during our experiments.

As for indicators of the stability of NLCs, the optimization parameters were measured after preparation (after 24 h), and also after one month (NLC1-8) and after one week (NLC9-16). On the basis of the results, the particle size of the NLC systems was less than 300 nm and the PDIs were less than 0.2, which means a narrow size distribution in all cases. The smallest particles and the narrowest size distributions were detected, where the total lipid concentration was low (10% w/w) and the surfactant concentration was high (5% w/w). The ZP values changed between 8 and 15, which corresponds to the literature data, where the ZP of NLC prepared with cremophor type emulsifier was about -12 mV[72]. These values, the low particle size and the narrow size distribution, can help to retain the stability of the nano systems. The EE% of the nano lipids was very high, over 87%, indicating the good drug loading capacity of the nano lipid carriers. EE% was better in the NLCs containing lower surfactant concentrations (NLCs 1-4), which may be explained by the appearance of the redundant surfactant in the aqueous phase, which can dissolve DXM in the aqueous phase in a higher amount.

When the samples were measured after 1 month, in two compositions the aggregation of the nano lipid particles resulted in the formation of a lipid cake on the top of the container, therefore none of the tested parameters could be measured in these cases. In the case of the homogenous samples, it could be observed that the PDI values remained within the narrow size. The absolute ZP values (if it was applicable) increased with storage time (after 1 month), which means the aqueous-lipid interface changed and became more stable after 1 month.

A mathematical model was used to analyse the single and combined effect of the factors. The coefficients in the equations describe the size and direction (negative: inversely proportional; or positive: directly proportional) of the relationship between a term in the

model and the response variable[73]. The mathematical model is shown in the following equations (Eqs (5)-(8)) of the response surfaces:

$$EE\% = 91.7 + 0.03\ A - 1.39\ B - 1.85\ C - 0.20\ AB - 0.28\ AC - 0.69\ BC\ , \quad (5)$$

$$Z_{ave}\ (d.nm) = 171.38 + 30.82\ A - 1.80\ B - 52.12\ C + 2.18\ AB - 3.96\ AC + 2.80\ BC\ , \quad (6)$$

$$PDI = 0.16 + 0.02\ A + 0.00\ B - 0.01\ C + 0.01\ AB + 0.01\ AC + 0.01\ BC\ , \quad (7)$$

$$ZP\ (mV) = -11.15 - 0.58\ A + 1.02\ B + 2.11\ C - 0.27\ AB + 0.20\ AC + 0.07\ BC \quad (8)$$

where factor A was lipid concentration, B was DXM concentration and C was surfactant concentration.

The results suggest that EE% depends on DXM and surfactant concentration (inversely proportional) as well. The combined effect of factors is also inversely related to EE%. On the basis of the coefficient value, the changes of entrapment efficiency are significant (higher coefficient values) with DXM concentration and surfactant concentration, while the combined effect of the factors is not remarkable (lower coefficient values). The mathematical model demonstrated that the lipid content does not influence EE% (very low coefficient value), so in this total lipid concentration range (10-15%) the drug loading capacity of NLCs cannot improve with increasing this concentration.

Z_{ave} is also affected by lipid (directly proportional), DXM and surfactant concentration (inversely proportional) but the amount of surfactant showed the most remarkable impact. The combined effect of factors is less expressed as it was observed in the case of EE%, too. The increase of the surfactant amount can be beneficial for particle size reduction, but as we could conclude from Eq 4., it can deteriorate drug loading capacity (lower EE% values).

Concerning PDI, very low coefficient values were calculated. In this case, the preparation technique and/or type of composition may have a more relevant influence on it, but these parameters were constant in our current experiments.

ZP is influenced by DXM, surfactant (directly related) and lipid concentration (inversely related). As it was concluded in the case of EE% and Z_{ave}, the combined effect of factors does not have a considerable effect on it. The most remarkable effect can be observed in the case of the surfactant, which means the increase in the surfactant concentration can improve the stability of NLCs (higher absolute ZP value), but higher values were found to reduce EE%.

As a conclusion, the surfactant concentration has the most remarkable effect on the stability parameter (Z_{ave} and ZP) of NLCs, an increased amount can be favourable, but we must bear in mind that its higher concentration can result in lower drug loading capacity and potential irritation and toxicity.

5.2.2.2. Mucoadhesive NLC formulation

To formulate a DXM containing mucoadhesive NLC system, hypromellose was applied as a mucoadhesive agent, which supposedly forms a gel layer around the nanoparticles. A 2^3 full factorial experimental design was used to optimize the mucoadhesive formulations. The chosen factors were polymer concentration (A), surfactant concentration (B), and DXM concentration (C). The optimization parameters (dependent factors) for the characterization of nanoparticles, the particle size (Z_{ave}), zeta potential (ZP), polydispersity index (PDI), d(0.1), d(0.5), d(0.9), Span value, entrapment efficacy (EE%) and mucoadhesivity of the NLC systems were chosen.

The polymer concentration is also essential because too high polymer concentrations can result in a gel form, which makes it impossible to use the formulation as an eye drop. However, the polymer is required to provide the lipid particles with a mucoadhesive effect. In our case the polymer has amphiphilic behaviour[74], therefore it can be present at the lipid-water interface in a higher concentration, thus resulting in a concentrated gel layer around the lipid particles. The polymer as a surfactant can modify the accumulation of other surfactants (e.g. Cremophors) at the interface, which may have an effect on the formation and stability of NLCs. The polymer concentration was also investigated at two levels (0.05% and 0.1%).

$$Z_{ave} = 153.22 \mathbf{- 4.93A} - \mathbf{42.65B} - \mathbf{1.74C} - \mathbf{5.50AB} + \mathbf{5.71AC} - 0.35BC, \quad (9)$$

$$PDI = 0.30 - 0.03A - 0.04B - 0.02C - 0.01AB + 0.04AC + 0.00BC, \quad (10)$$

$$ZP = -7.65+0.46A+2.21B-0.44C+0.24AB+0.83AC-1.49BC, \quad (11)$$

$$EE\% = 88.63 - 0.51A+3.6B+0.35C-0.69AB+0.51AC-1.18BC, \quad (12)$$

$$d(0.5) = 0.12 - 0.001A -0.003B + 0.002C + 0.000AB +0.000AC+0.002BC, \quad (13)$$

$$\text{Span value}=1.24-0.05A-0.1B+0.11C-0.09AB+0.01AC+0.1BC. \quad (14)$$

Equations (9-14) show the effect of the chosen factors on the optimization parameters and the combined factors on optimization parameters (Zave, PDI, ZP, EE%, d(0.5) and Span value). The bold values in the equations indicate a significant effect.

Table 4. *The particle size, polydispersity index, zeta potential, and entrapment efficacy of the mucoadhesive NLC compositions (mean and ± SD)*

	After 1 day				After 1 week		
	Z_{ave} (d.nm)	**PDI**	**ZP (mV)**	**EE %**	**Z_{ave} (d.nm)**	**PDI**	**ZP (mV)**
NLC9	202.33±0.70	0.42±0.008	-9.95±0.27	83.50	285.67± 4.06	0.55 0.01±	-10.00± 0.26
NLC10	192.17±2.86	0.30±0.040	-11.87±0.40	83.47	241.13± 1.80	0.46± 0.02	-9.24± 0.19
NLC11	128.87±3.96	0.35±0.015	-3.73±0.17	95.07	141.07± 1.86	0.46± 0.02	-13.30± 0.26
NLC12	96.46±0.63	0.20±0.006	-3.29±0.36	91.06	122.50± 0.50	0.43± 0.01	-4.91± 0.60
NLC13	188.27±2.70	0.29±0.006	-10.20±0.10	86.19	264.77± 7.21	0.49± 0.02	-9.40± 0.18
NLC14	200.70±7.63	0.34±0.039	-7.41±0.06	86.94	270.07± 6.66	0.49± 0.03	-15.77± 0.57
NLC15	113.13±0.81	0.25±0.005	-8.55±0.19	91.78	143.63± 3.97	0.44± 0.04	-9.50± 0.57
NLC16	103.83±0.46	0.23±0.006	-6.19±0.17	91.02	137.83± 0.38	0.45± 0.01	-7.66± 0.24

Table 5. *The results of laser diffraction based particle size analysis*

	After 1 day				After 1 week			
	d (0.1)	**d (0.5)**	**d (0.9)**	**Span value**	**d (0.1)**	**d (0.5)**	**d (0.9)**	**Span value**
NLC9	0.075	0.125	0.245	1.355	0.107	1.523	44.681	29.269
NLC10	0.071	0.122	0.229	1.293	0.091	0.303	35.697	117.694
NLC11	0.074	0.113	0.190	1.026	0.066	0.135	1.123	7.819
NLC12	0.075	0.111	0.168	0.831	0.063	0.122	0.244	1.486
NLC13	0.074	0.123	0.227	1.241	0.097	0.415	39.093	93.901
NLC14	0.070	0.122	0.248	1.461	0.097	0.393	36.777	93.387
NLC15	0.079	0.123	0.266	1.532	0.087	0.266	13.672	51.152
NLC16	0.074	0.118	0.212	1.169	0.065	0.130	0.525	3.521

Based on the results (Table 4, 5) of the factorial design, surfactant concentration, polymer concentration and DXM concentration have a significant effect on Z_{ave} (eq. 9). The combined effects of the polymer and surfactant concentration (AC), and the polymer and DXM concentration (AB) also have a significant effect on Z_{ave}. Based on the coefficient values, the surfactant concentration, polymer concentrations and DXM concentrations are inversely related to particle size (eq. 9,13), which means that the increase in the concentration of the above-mentioned components decreases the particle size of the nanocarriers.

After one week the particle size of all compositions increased. The slight increase of Z_{ave} can be explained by the formation of a gel layer around the particle, while the remarkable

change in the d(0.5), d(0.9) and Span values can indicate the aggregation of the lipid particles via the gel surfaces. In the case of NLC12 and NLC16, the increase in the d(0.5), d(0.9), and Span values were not remarkably higher compared with the other formulations, which can mean that the particles of NLC12 and NLC16 do not aggregate so much even after one week. On the other hand, the Z_{ave} value of NLC12 and 16 increased to the same extent as for the other formulations suggesting the formation of a gel layer around the nanoparticles in each composition. NLC12, 16 contain a higher amount of surfactant and polymer, and their combination can result in a more stable interfacial layer.

The compositions with a higher surfactant concentration (NLC11, 12 and NLC15, 16) have a lower absolute ZP value. However, after one week, if the surfactant concentration is higher, ZP will be higher (of absolute value) as well. The reason for this might be that the formation of the final interface structure takes more time than one day.

The formulations with a lower surfactant concentration (NLC9, 10 and NLC13, 14) have lower entrapment efficiency. This finding suggests a higher surfactant concentration is needed to dissolve and entrap DXM in the lipid carriers, 5% of surfactant can result in high, more than 90% EE%.

The absolute ZP value of the nanoparticulate system is quite low, but on the basis of our results, the preparation with the lowest absolute ZP values showed the highest stability (considering the Z_{ave}, PDI, d(0.5) and Span values), which can suggest our polymer-surfactant containing systems are mainly sterically stabilized.

5.2.3. Mucoadhesion study

In order to improve the mucoadhesivity of the formulations, a mucoadhesive polymer, hypromellose was added to the NLC systems. Hypromellose is a safe mucoadhesive polymer often used in ophthalmic formulations [75]. The applied concentrations were 0.05 w/w% and 0.1 w/w% because higher polymer content resulted in the creaming of the nano-formulation.

Because of its surface-active property[76], hypromellose may accumulate at the lipid-water interface, resulting in a concentrated gel layer around the particles. This gel layer can attach each particle separately to the mucosal surface. The mucoadhesion of the NLC compositions was compared with the same compositions without hypromellose and then statistical analysis (T-test) was applied to evaluate the significance. It was found that there is a significant difference between samples with and without the mucoadhesive polymer (Fig. 11) in the case of most compositions. Generally, the samples containing a higher surfactant amount (5%) (NLC11 and 12) displayed higher adhesive work values than the compositions with a lower surfactant amount, which can mean remarkable mucoadhesivity even without adhesive polymers. The possible cause of this phenomenon is the different interfacial layer.

In these formulations, the addition of the polymer did not change the mucoadhesivity, which can be explained by the fact that the high surfactant concentration limits the orientation of the polymer to the surface of the NLCs. In our compositions, the polymer concentration did not change mucoadhesivity in the investigated polymer concentration range, there was no significant difference between the samples containing 0.05 w/w% and 0.10 w/w% polymer, which could be explained by the saturated interface of the NLCs even at a low polymer concentration.

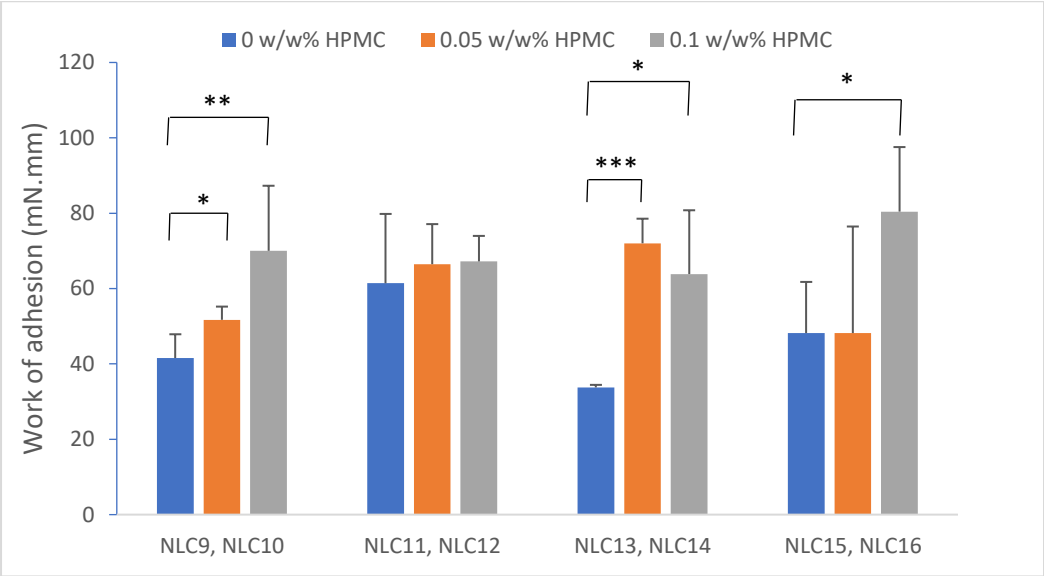

***Figure 11**. Comparison of mucoadhesion of the NLCs with and without polymer*

5.2.4. In vitro drug release study

5.2.4.1. Investigation of basic NLC formulations

In order to compare our optimized NLCs with the conventional suspension form, *in vitro* drug release studies were performed. On the basis of the results of our factorial experimental design, the four most relevant compositions were chosen to be compared with 0.1% DXM suspension. Two of the chosen compositions (NLC3 and 7) contained the same concentration of DXM (0.10%) as in the case of the suspension, while two of them (NLC1 and 5) contained half the amount (0.05%) of that. The drug release profile of the formulations was analysed in Table 6.

***Table 6**. Summary of the drug release study: the rate constant (K) and the correlation coefficient (R^2) of the Higuchi model, the amount of the released DXM at 6 hours of the release study; and the results of the statistical analysis, where the NLCs were compared with the DXM suspension.*

Formulation	Higuchi model		Released DXM at 6h (µg)	Results of the statistical analysis
	K	R^2		
DXM Suspension	3.69	0.9836	68.5±4,5	reference system
NLC1	3.65	0.9967	56.7±4,8	highly significant ($p \leq 0.001$) from 0.5 h
NLC3	6.73	0.9940	104.2±5,2	highly significant ($p \leq 0.001$) from 3 h
NLC5	4.68	0.9971	76.2±0,2	significant ($p \leq 0.05$) at 6 h
NLC7	9.26	0.9968	140.5±0,2	highly significant ($p \leq 0.001$) from 1 h

The mathematical modelling of the *in vitro* release data showed the DXM release from NLCs and the suspension followed Higuchi release kinetics (R^2 is higher than 0.99 for NLCs and higher than 0.98 for suspension). This type of kinetic indicates a diffusion-controlled release from the systems. It could be seen that the NLCs containing 0.10% DXM showed a remarkable drug release. These results can predict a 100% increase in drug release using NLC7. When we consider the NLCs containing 0.05% DXM, the NLC1 composition displayed a lower amount of the released drug at each time point, while the NLC5 composition was similar to the suspension form (no significant differences during the drug release, except at 6 hours, where a significantly higher drug amount was detected in the case of NLC5). This finding can also confirm that the NLC composition can increase the amount of the released drug (Fig. 12.).

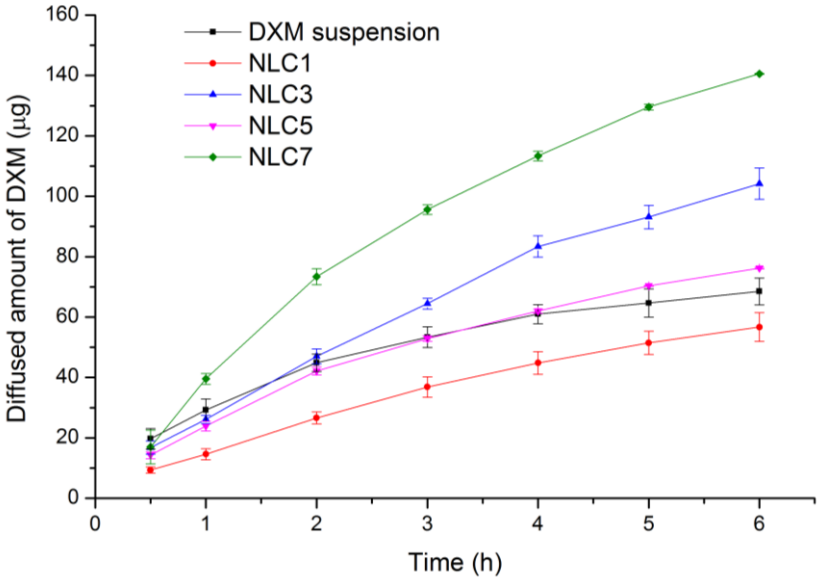

***Figure 12**. In vitro drug release from NLC formulations (NLC1, 3, 5, 7) and DXM suspension.*

5.2.4.2. Investigation of NLC formulations

The *in vitro* drug release from hypromellose containing NLC systems were also investigated. The compositions were the same as in the factorial experimental design (NLC9-16).

Considering the results of the factorial design, we can conclude that the emulsifier and the DXM concentration have a significant effect (significant factors are indicated in bold) on drug diffusion (diffused drug amount at 6h, ($C_{DXM\ (6h)}$)). The surfactant concentration (B) has a significant negative effect on diffusion (eq. 12), whereas the DXM concentration (C) has a significant positive effect on diffusion.

$$C_{DXM\ (6h)} = 73.50 + 1.64A \mathbf{- 14.40B + 25.07C} - 1.24AB + 2.65AC - 3.11BC, \quad (12)$$

The highest diffused amount of DXM could be detected in the case of NLC13 and 14 (Figure 13) both of which contain a lower amount of surfactant, and have the lowest entrapment efficiency (Table 4.). This finding could show us that if less API is entrapped in the nanocarriers (more free DXM), a higher amount will diffuse through the synthetic membrane, and on the other hand, it can mean that the high emulsifier concentration (and/or high entrapment efficiency) in the system can have a restraining effect on DXM diffusion. At lower drug contents (NLC9-12 and 0.5% DXM suspension), the dilution of the acceptor phase during sampling can result in the total dissolution of DXM from the suspension form, while the incorporation into a lipid carrier with high entrapment efficiency can hinder this process of dissolution into the medium (as it was mentioned above). That is why we could observe a lower diffusion rate in our NLC formulations which contain a high surfactant and a low API amount, compared with the conventional suspension form. This could explain why NLC11 and 12 with higher entrapment efficacy showed the lowest diffused amount of DXM (Table 4).

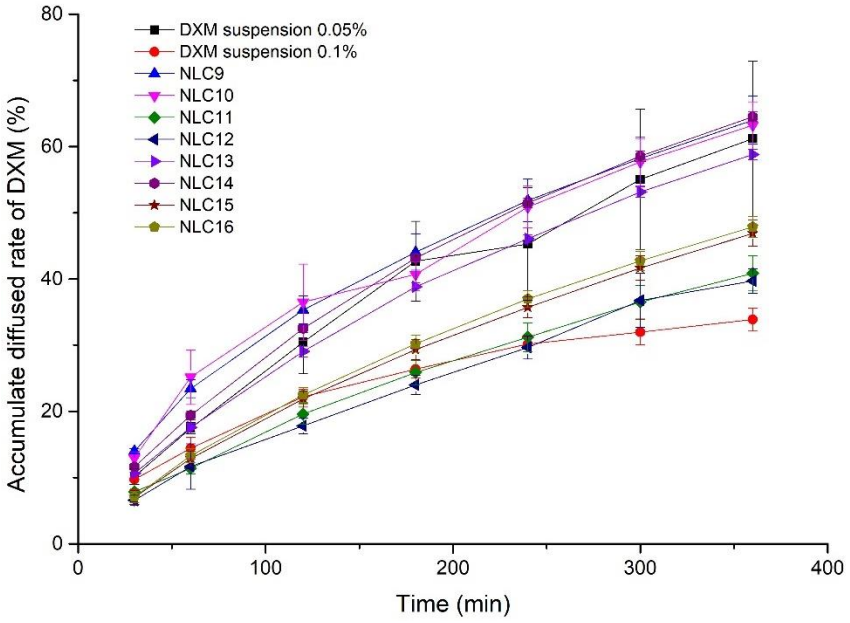

Figure 13*. The diffused amount of DXM from NLC compositions through the dialysis membrane.*

5.2.5. Cell viability assay

5.2.5.1. NLC formulations

In order to analyse the possible toxicity of the formulated NLCs, a human cornea cell viability study was applied, where the most relevant compositions based on the drug release study, the emulsifier (Cremophor RH60), and DXM were investigated using MTT assay[18].

During the colorimetric assay, NLC3 and NLC7 formulations at 10× dilution slightly decreased the viability of the HCE-T cells after 6-hour treatment. The 100× dilutions did not cause any significant alteration in the cell index, indicating no cell damage. Cremophor RH60 did not reduce the cell viability of epithelial cells neither at 2.5 mg/mL nor at 5 mg/mL concentration for 6 hours. These results are in accordance with our previous studies, where concentrations of Cremophor RH40 less than 10 mg/mL were non-toxic for different cultured epithelial cells[77,78].

5.2.5.2. Mucoadhesive NLC formulations

The full NLC formulations (NLC9-12) and the polymer alone were evaluated using impedance measurement. Real-time cell electronic sensing is a non-invasive, label-free, impedance-based technique to quantify the kinetics of proliferation, viability, and the cellular reaction of adherent cells. This method can be successfully used to follow cell damage and/or protection in living barrier-forming cells[61,79].

The impedance measurements did not show significant cell damage after treatment with different DXM containing NLC formulations. As a comparison, cells treated with the reference molecule Triton X-100 were lysed and impedance dropped to a minimum. DXM

exerted a cell layer tightening effect that is visible in all NLC treatment groups as an increased level of impedance[80,81].

Hypromellose did not significantly change the cell index of HCE-T cells, which indicates no cytotoxic effect on this cell type. The reference compound, Triton X-100 detergent caused cell death, as reflected by the decrease in impedance.

5.2.6. Immunohistochemistry

The cell viability test was supplemented with immunohistochemistry in order to clarify the effect of the formulations on the barrier function of human corneal epithelial cell layers. No major morphological changes were observed in the treated groups. All junctional proteins were localized at the intercellular connections forming continuous pericellular belts in every group [56].

5.2.7. Penetration studies

Permeability is the ability of drug molecules to penetrate through the biological membranes. In our study, 3 different methods were applied and compared with each other: *in vitro* high throughput corneal-PAMPA; permeability study on cell culture; and *ex vivo* penetration study on porcine cornea followed by Raman correlation mapping.

5.2.7.1. Application of corneal-PAMPA model

In order to get more information about the expected amount of penetrated DXM through the cornea, a parallel artificial membrane permeability assay (PAMPA) was used. On the basis of literature data, cornea-PAMPA can be successfully applied for the penetration study of ocular APIs as a fast, cost-effective screening method[60]. In our study, the penetration of DXM in different NLCs was evaluated and compared with DXM suspension (0.1%) in order to find a correlation between the composition and the penetration ability of DXM (Fig. 14. a.). The highest penetrated DXM amount was detectable in the case of NLC11, 12, 13 and 14, and there was no significant difference between the penetrated amount of DXM in the case of DXM suspension and NLC9-16.

More relevant information can be concluded when the flux values are considered, in this case, the donor concentration of the applied formulations is considered. The comparison of the flux values of the NLC systems with the suspension indicated remarkable penetration when DXM was incorporated in nanocarriers (Fig. 14.b.). Surprisingly, NLC11 and 12 showed the highest penetration and a highly significant difference from the DXM suspension form. However, the NLC11 and 12 formulations showed a lower drug diffusion during the *in vitro* drug diffusion study. This contradiction may be explained by the interaction between the components of the NLCs and the cornea-PAMPA membrane. The applied emulsifier and

lipids can modify the permeability of the impregnated PAMPA membrane, resulting in improved penetration. The largest alteration between the PAMPA and the *in vitro* drug diffusion study can be observed in the case of the compositions with higher surfactant concentration, which can suggest the interaction occurs between the emulsifier and the membrane, resulting in improved PAMPA penetration[56].

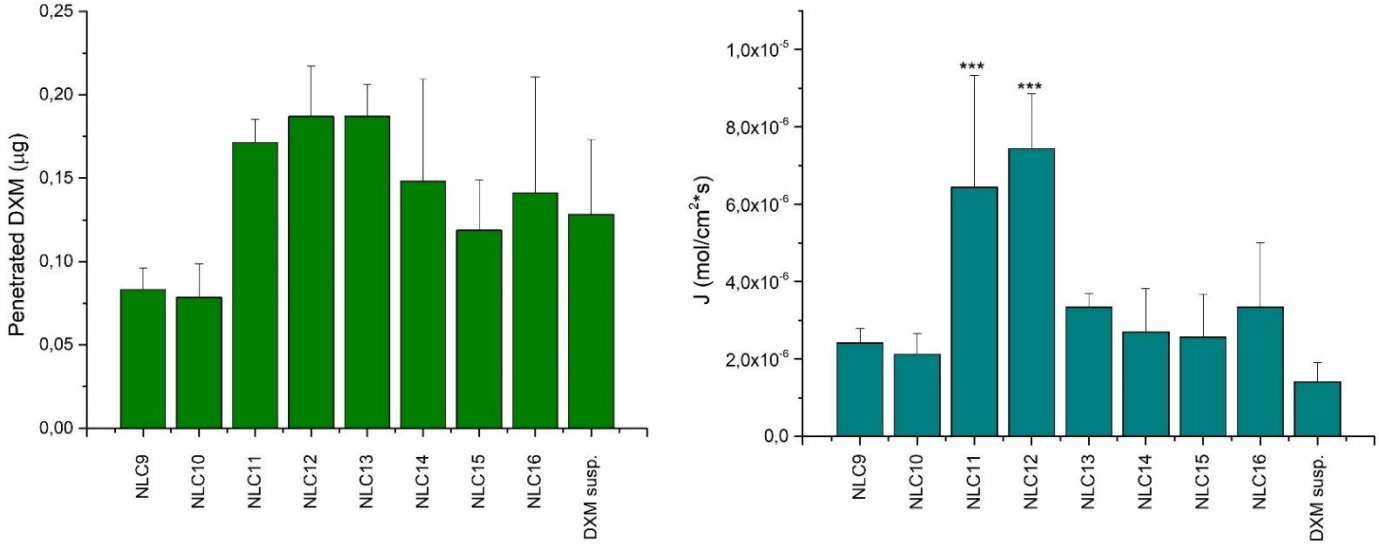

a) b)

Figure 14*. a) Comparison of the diffused amounts of DXM through Corneal-PAMPA model b) The flux of DXM from the NLC systems through corneal-PAMPA model.*

5.2.7.2. Permeability study on cell culture model

The permeability of DXM from suspension and different NLC formulations was tested on the HCE-T cell model as well. It can be seen that the highest amount diffused in the case of the NLC13 and NLC14 formulations, while the NLC15 and NLC16 formulations showed a lower amount of diffused DXM (Fig. 15.). After 60 minutes, the diffused amount of DXM was significantly higher for NLC6 than for the suspension form. When there was a higher free concentration in the donor phase, the amount of diffused DXM was also higher. This tendency is similar to that in the case of in vitro drug diffusion study. This may suggest that if the entrapment efficiency is higher, a lower amount of DXM can diffuse from the NLC systems.

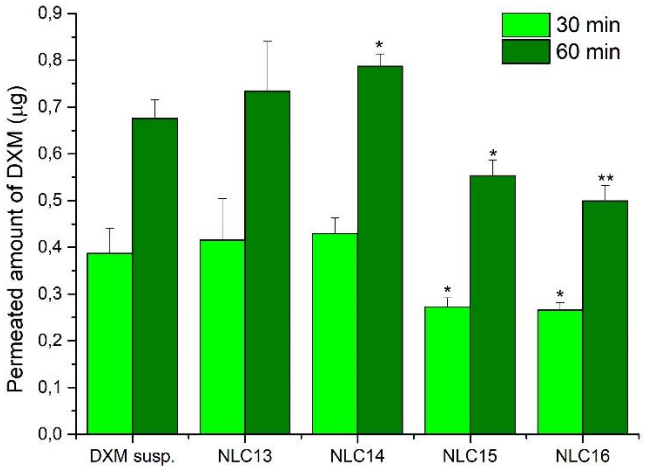

***Figure 15**. The penetrated amount of DXM through HCE-T cells after 30 min and 60 min. Values are presented as means ± SD. Statistical analysis: ANOVA followed by Dunnett's test.*

Considering the permeability (P_{app}) values after treatment, all NLC formulations showed higher values compared to the suspension, which indicates a better penetration of the API when using nano lipid compositions (Fig. 16).

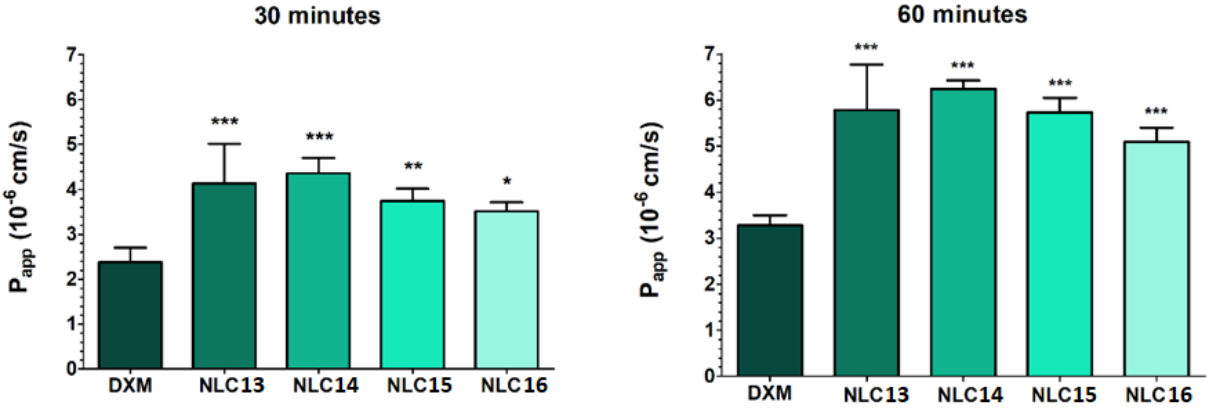

***Figure 16**. Apparent permeability coefficients (P_{app}) for DXM suspension (DXM) or in different formulations (NLC) measured across HCE-T corneal epithelial cell layers after 30 and 60 minutes of incubation. Values are presented as means ± SD, n = 4/group. Statistical analysis: ANOVA followed by Dunnett's test.*

The barrier properties were investigated measuring the TEER values after the permeability study. HCE-T cell layers showed high TEER values indicating tight barrier properties and suitability for the permeability assay. The different formulations did not change the TEER values significantly compared to the relevant control groups, suggesting no damaging effects of the formulations on the epithelial cell layers.

These good barrier properties were confirmed with the permeability measurements of different indicator molecules (fluorescein and albumin). These values show that the epithelial

barrier was not affected by the formulations, as it was also presented in the immunohistochemistry assay earlier[56].

5.2.7.3. Correlation between the different penetration models

In order to evaluate the penetration studies, the correlation of the penetrated amount of drug through different membranes was analysed. Correlated results may confirm the relevance and applicability of the models and can help to choose the most suitable one to predict the bioavailability of the API in NLCs.

The results of the *in vitro* diffusion study and penetrated amount of DXM though Corneal-PAMPA does not correlate with each other (Figure 17.a.). The correlation coefficient was 0.06522, which means that there is no correlation between the results of penetration and diffusion studies.

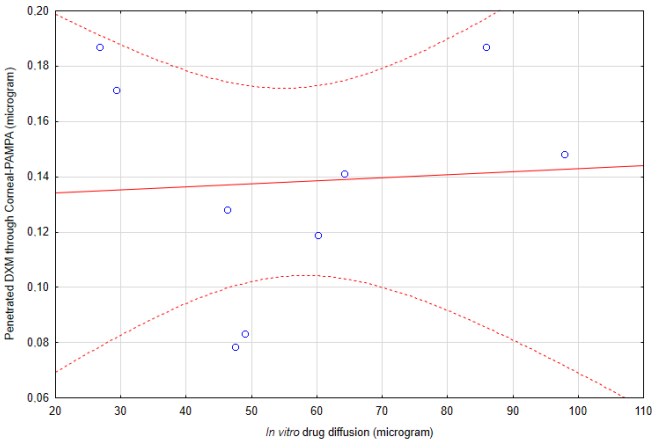

a)

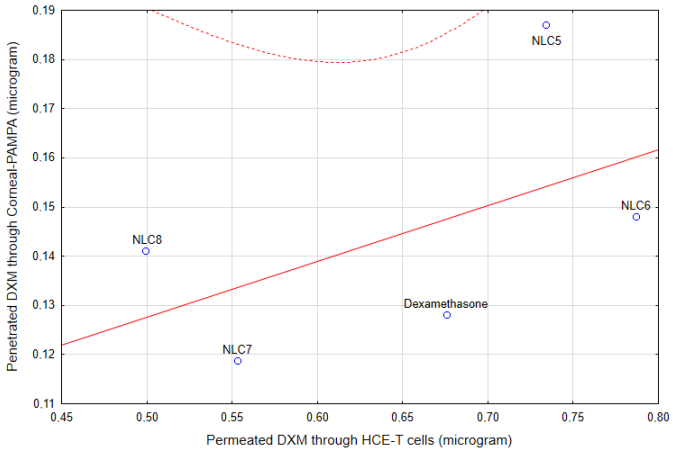

b)

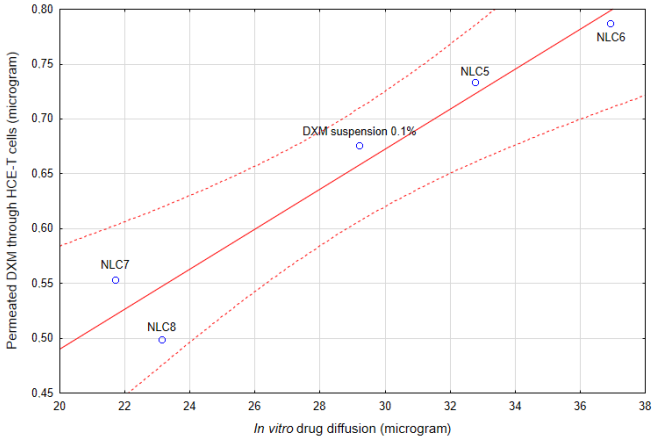

c)

Figure 17. *a) The correlation of in vitro diffusion study and penetrated the amount of DXM through Corneal-PAMPA, b) The correlation of HCE-T cell line permeability and the Corneal-PAMPA model, c) The correlation of in vitro diffusion study and HCE-T cell line permeability*

The correlation coefficient between the results of penetrated DXM though HCE-T cells and the penetrated amount though Corneal-PAMPA is 0.52248, which indicates a moderate correlation [82] between these two models (Figure 17.b.). However, as it was mentioned above, the component of the NLC can modify the PAMPA membrane, which can alter the permeability in this model, while the cell membrane remained the same in the case of cell penetration study, which can explain this moderate correlation.

Surprisingly, the correlation between the *in vitro* diffusion study and the HCE-T cell line permeability study was very high (Figure 17.c.). The correlation coefficient was 0.96595, which indicates a strong correlation. As it was presented, the formulations did not change the barrier function of the corneal epithelial cells (immunohistochemistry, P_{app} of fluorescein and albumin), the main rate-limiting factor for the penetration of DXM in NLC formulations is the drug release from the nanocarriers.

The correlation study indicated altered results for the PAMPA model, namely the applied surfactant and lipid can modify the PAMPA membrane, which can result in inappropriate conclusions. This observation can highlight the possible limited applicability of the corneal-PAMPA model in the case of lipid compositions.

As a practical conclusion, in the future, the *in vitro* drug release study can offer a possibility to compare the bioavailability of the further modifications of this type of NLCs.

5.2.7.4. Ex vivo Raman correlation mapping

Based on the drug diffusion study and the cell line penetration test, NLC14 was selected for the semi-quantitative Raman mapping examination. The porcine corneas were treated with the formulations with (NLC14), and without polymer. Specimens were created from the treated and non-treated cornea as well. A specimen treated with NLC14 and its polymer-free version were compared with a non-treated cornea specimen. The spectrum of NLC14 was used for the cornea distribution correlation maps, except in the case of the polymer-free formulation treated cornea specimen, when its spectrum was applied for creating the correlation map (Figure 17). In the case of the polymer-free NLC, we can observe a significant amount of components (surfactant and lipids) of NLCs in the stroma layer (300 μm penetration depth) of the cornea. On the basis of the Raman correlation map, we could not distinguish which components were diffused. Tian et al.[83] analysed the penetration of NLCs trough cornea, they established that NLCs do not penetrate directly into the cornea, but some of the components can be detected in it.

As for the polymer containing NLC (NLC14), Raman intensity is remarkable on the surface of the cornea and in the upper part of the stroma. However, in the case of the polymer-free NLC, Raman intensity is stronger in the upper part of the stroma. Thanks to its adhesive

properties, NLC14 might form a very significant depot on the corneal surface, and it presented fewer transitions of components through the epithelial layer into the hydrophilic stroma. The accumulation of the hydrophilic polymer at the nano lipid carrier surface can change the polarity of the lipid surface and can increase the particle size, therefore, these modifications can lead to lower but still remarkable penetration of some NLC components across the lipophilic corneal epithelial cells.

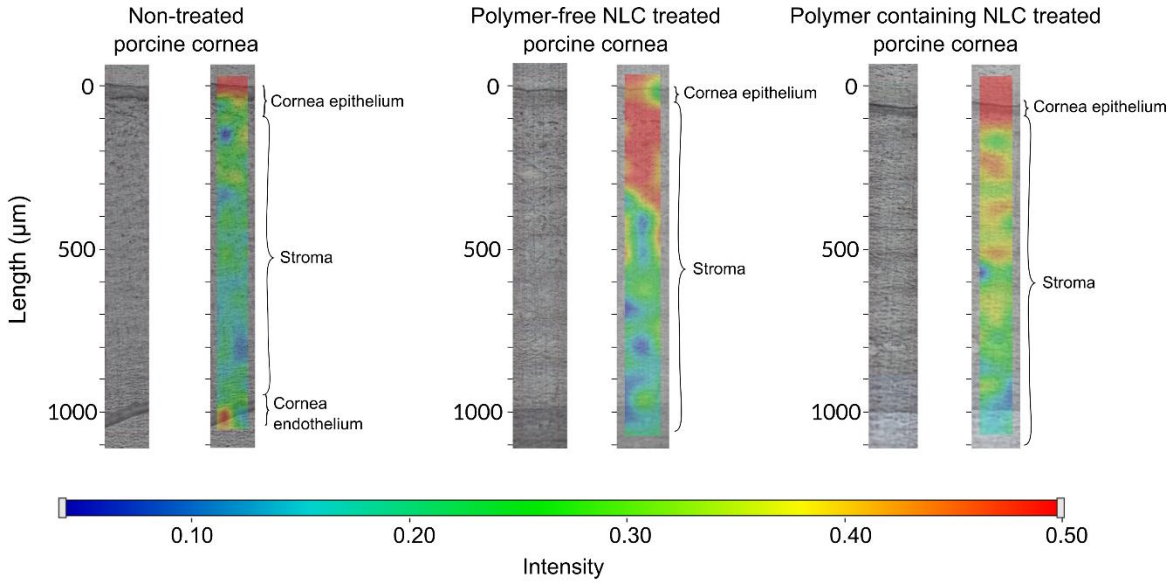

Figure 17*. The Raman correlation map of NLC14 and the polymer-free version of the composition.*

5.2.8. Conclusion

Successful formulation of non-toxic potential ophthalmic NLC systems has been achieved with a narrow size distribution, high DXM entrapment efficiency, and increased penetration. The chosen components were Compritol 888 ATO, Miglyol 812N and Cremophor RH60. The use of low surfactant and lipid concentrations is recommended (e.g. 2.5% for surfactant and 10% for total lipids) because then the critical stability parameters (Zave, ZP, PDI) and drug loading (EE%) are adequate, while the concentration of the emulsifier may remain low.

In the second part of my PhD work, we successfully combined mucoadhesive polymers with DXM-loaded NLCs. Based on the results of mucoadhesive studies, the incorporation of hypromellose even at low polymer concentrations increased the mucoadhesive properties compared to non-polymeric formulations.

Characterization of the nanoparticles (Z_{ave}, PDI, d (0.5), and Span values) showed that the formulation with the lowest absolute ZP value had the highest stability, suggesting that our systems containing the polymeric surfactant were primarily sterically stabilized.

The biocompatibility of NLC systems was evaluated by toxicity tests on HCE-T cells, impedance measurements, and immunoassays. These measurements showed, there was no cell damage after treatment and the formulations had no adverse effects on cell nodes.

Examination of DXM drug release compared to conventional suspension forms showed increased drug diffusion from NLC systems, and it could also be concluded that a formulation with a very high entrapment efficiency could inhibit drug release from particles. These results were in correlation with the cell permeability assays, where the optimized NLCs presented significantly better permeability across HCE-T cells.

The mucoadhesivity and penetration enhancing effects of our NLCs were demonstrated in an *ex vivo* penetration study in the porcine cornea by Raman correlation mapping. Untreated and treated (with and without polymer) porcine corneas were compared. The results showed that NLC systems containing hypromellose polymers could create a depot on the corneal surface. This may suggest sustained release and longer residence time of DXM using this type of polymer-modified NLC systems.

6. SUMMARY

My PhD work aimed to formulate innovative drug delivery systems for ophthalmic use. The novelty of this work can be summarized as follows:

- Formulation of *in situ* gelling delivery with the cyclodextrin modified thiolated polymer, which can make it possible to incorporate prednisolone as the active ingredient in a hydrophilic mucoadhesive ophthalmic composition.
- The binding of cyclodextrin to the polymer increased the duration of the effect and became programmable by changing the ratios of the free and bound forms of the cyclodextrin.
- The optimal composition of DXM loaded mucoadhesive NLC systems, which increased the possible residence time on the eye surface, was first described.
- The biocompatibility of chosen components to formulate NLC systems were verified with the immunohistochemistry method and cell viability assay.
- The correlation of the in vitro drug release study and permeability study (on HCE-T cells and corneal-PAMPA) of the ophthalmic formulations were investigated, and a strong correlation was found between in vitro drug release study and permeability on HCE-T cells.
- *Ex vivo* Raman mapping was applied in order to follow the penetration trough cornea, and it was proved that the components of basic NLC formulations could penetrate the

stroma layer, while in the case of polymer containing NLC formulations, the system could create a depot on the eye surface.

To sum up, it can be concluded that the thiolated mucoadhesive hydrogels and NLCs described in the thesis have the possibility to increase the bioavailability of the ophthalmic steroidal anti-inflammatory drug.

7. REFERENCES

1. *Mucosal delivery of biopharmaceuticals: biology, challenges and strategies*. (Springer, 2014).
2. Gan, L. *et al.* Recent advances in topical ophthalmic drug delivery with lipid-based nanocarriers. *Drug Discov. Today* **18**, 290–297 (2013).
3. Omidi, Y. *et al.* Evaluation of the immortalised mouse brain capillary endothelial cell line, b.End3, as an in vitro blood-brain barrier model for drug uptake and transport studies. *Brain Res.* **990**, 95–112 (2003).
4. Smith, M., Omidi, Y. & Gumbleton, M. Primary porcine brain microvascular endothelial cells: Biochemical and functional characterisation as a model for drug transport and targeting. *J. Drug Target.* **15**, 253–268 (2007).
5. Barar, J., Javadzadeh, A. R. & Omidi, Y. Ocular novel drug delivery: impacts of membranes and barriers. *Expert Opin. Drug Deliv.* **5**, 567–581 (2008).
6. Kamaleddin, M. A. Nano-ophthalmology: Applications and considerations. *Nanomedicine Nanotechnol. Biol. Med.* **13**, 1459–1472 (2017).
7. Jiao, J. Polyoxyethylated nonionic surfactants and their applications in topical ocular drug delivery. *Advanced Drug Delivery Reviews* vol. 60 1663–1673 (2008).
8. Lawrence, M. J. & Rees, G. D. Microemulsion-based media as novel drug delivery systems. *Adv. Drug Deliv. Rev.* **64**, 175–193 (2012).
9. Vandamme, Th. F. Microemulsions as ocular drug delivery systems: recent developments and future challenges. *Prog. Retin. Eye Res.* **21**, 15–34 (2002).
10. Trivedi, R. & Kompella, U. B. Nanomicellar formulations for sustained drug delivery: strategies and underlying principles. *Nanomed.* **5**, 485–505 (2010).
11. Civiale, C., Licciardi, M., Cavallaro, G., Giammona, G. & Mazzone, M. G. Polyhydroxyethylaspartamide-based micelles for ocular drug delivery. *Int. J. Pharm.* **378**, 177–186 (2009).
12. Ideta, R. *et al.* Effective accumulation of polyion complex micelle to experimental choroidal neovascularization in rats. *FEBS Lett.* **557**, 21–25 (2004).
13. Pescina, S., Sonvico, F., Santi, P. & Nicoli, S. Therapeutics and carriers: the dual role of proteins in nanoparticles for ocular delivery. *Curr. Top. Med. Chem.* **15**, 369–385 (2015).
14. Ludwig, A. The use of mucoadhesive polymers in ocular drug delivery. *Adv. Drug Deliv. Rev.* **57**, 1595–1639 (2005).
15. Calvo, P., Vila-Jato, J. L. & Alonso, M. J. Evaluation of cationic polymer-coated nanocapsules as ocular drug carriers. *Int. J. Pharm.* **153**, 41–50 (1997).
16. Maity, P., Moin, A., Gowda, D. V. & Osmani, R. A. M. Ophthalmic drug delivery by contact lenses. *Journal of Chemical and Pharmaceutical Research* vol. 8 644–651 (2016).
17. Zhang, R. *et al.* Treatment of experimental autoimmune uveoretinitis with intravitreal injection of tacrolimus (FK506) encapsulated in liposomes. *Invest. Ophthalmol. Vis. Sci.* **51**, 3575–3582 (2010).
18. Souto, E. B., Doktorovova, S., Gonzalez-Mira, E., Egea, M. A. & Garcia, M. L. Feasibility of Lipid Nanoparticles for Ocular Delivery of Anti-Inflammatory Drugs. *Curr. Eye Res.* **35**, 537–552 (2010).
19. Gan, L. *et al.* Recent advances in topical ophthalmic drug delivery with lipid-based nanocarriers. *Drug Discov. Today* **18**, 290–297 (2013).
20. Khosa, A., Reddi, S. & Saha, R. N. Nanostructured lipid carriers for site-specific drug delivery. *Biomed. Pharmacother.* **103**, 598–613 (2018).
21. Li, X. *et al.* A controlled-release ocular delivery system for ibuprofen based on nanostructured lipid carriers. *Int. J. Pharm.* **363**, 177–182 (2008).

22. Gonzalez-Mira, E., Egea, M. A., Garcia, M. L. & Souto, E. B. Design and ocular tolerance of flurbiprofen loaded ultrasound-engineered NLC. *Colloids Surf. B Biointerfaces* **81**, 412–421 (2010).
23. Balguri, S. P., Adelli, G. R. & Majumdar, S. Topical ophthalmic lipid nanoparticle formulations (SLN, NLC) of indomethacin for delivery to the posterior segment ocular tissues. *Eur. J. Pharm. Biopharm.* **109**, 224–235 (2016).
24. Araújo, J., Nikolic, S., Egea, M. A., Souto, E. B. & Garcia, M. L. Nanostructured lipid carriers for triamcinolone acetonide delivery to the posterior segment of the eye. *Colloids Surf. B Biointerfaces* **88**, 150–157 (2011).
25. Mo, Z. *et al.* Nanostructured lipid carriers-based thermosensitive eye drops for enhanced, sustained delivery of dexamethasone. *Nanomed.* **13**, 1239–1253 (2018).
26. Kassem, M. A., Abdel Rahman, A. A., Ghorab, M. M., Ahmed, M. B. & Khalil, R. M. Nanosuspension as an ophthalmic delivery system for certain glucocorticoid drugs. *Int. J. Pharm.* **340**, 126–133 (2007).
27. Ali, H. S. M., York, P., Ali, A. M. A. & Blagden, N. Hydrocortisone nanosuspensions for ophthalmic delivery: A comparative study between microfluidic nanoprecipitation and wet milling. *J. Control. Release Off. J. Control. Release Soc.* **149**, 175–181 (2011).
28. Ahmed, E. M. Hydrogel: Preparation, characterization, and applications: A review. *Journal of Advanced Research* vol. 6 105–121 (2015).
29. Hennink, W. E. & van Nostrum, C. F. Novel crosslinking methods to design hydrogels. *Adv. Drug Deliv. Rev.* **64**, 223–236 (2012).
30. Joglekar, M. & Trewyn, B. G. Polymer-based stimuli-responsive nanosystems for biomedical applications. *Biotechnology Journal* vol. 8 931–945 (2013).
31. Deligkaris, K., Tadele, T. S., Olthuis, W. & van den Berg, A. Hydrogel-based devices for biomedical applications. *Sensors and Actuators, B: Chemical* vol. 147 765–774 (2010).
32. Casolaro, M., Casolaro, I. & Lamponi, S. Stimuli-responsive hydrogels for controlled pilocarpine ocular delivery. *Eur. J. Pharm. Biopharm.* **80**, 553–561 (2012).
33. Radhakrishnan, J., Krishnan, U. M. & Sethuraman, S. Hydrogel based injectable scaffolds for cardiac tissue regeneration. *Biotechnol. Adv.* **32**, 449–461 (2014).
34. Geethalakshmi, A., Karki, R., Sagi, P., Jha, S. K. & Venkatesh, D. P. Temperature triggered in situ gelling system for betaxolol in glaucoma. *J. Appl. Pharm. Sci.* **3**, 153–159 (2013).
35. Almeida, H., Amaral, M. H., Lobão, P. & Lobo, J. M. S. In situ gelling systems: A strategy to improve the bioavailability of ophthalmic pharmaceutical formulations. *Drug Discov. Today* **19**, 400–412 (2014).
36. Park, B. K. & Kim, M. M. Applications of chitin and its derivatives in biological medicine. *International Journal of Molecular Sciences* vol. 11 5152–5164 (2010).
37. Chenite, A., Buschmann, M., Wang, D., Chaput, C. & Kandani, N. Rheological characterisation of thermogelling chitosan / glycerol-phosphate solutions. *Carbohydr. Polym.* **46**, 39–47 (2001).
38. Cho, J., Heuzey, M. C., Bégin, A. & Carreau, P. J. Physical gelation of chitosan in the presence of β-glycerophosphate: The effect of temperature. *Biomacromolecules* **6**, 3267–3275 (2005).
39. Ruel-Gariépy, E. & Leroux, J.-C. In situ-forming hydrogels—review of temperature-sensitive systems. *Eur. J. Pharm. Biopharm.* **58**, 409–426 (2004).
40. Loh, X. J. *et al.* New thermogelling poly(ether carbonate urethane)s based on pluronics F127 and poly(polytetrahydrofuran carbonate). *J. Appl. Polym. Sci.* **131**, n/a-n/a (2014).
41. You, J.-O., Almeda, D., Ye, G. J. & Auguste, D. T. Bioresponsive matrices in drug delivery. *J. Biol. Eng.* **4**, 15 (2010).
42. Yoshida, T., Lai, T. C., Kwon, G. S. & Sako, K. pH- and ion-sensitive polymers for drug delivery. *Expert Opin. Drug Deliv.* **10**, 1497–1513 (2013).

43. Bernkop-Schnürch, A. & Greimel, A. Thiomers: The new generation of mucoadhesive polymers. *American Journal of Drug Delivery* vol. 3 141–154 (2005).
44. El-Kamel, A. H. In vitro and in vivo evaluation of Pluronic F127-based ocular delivery system for timolol maleate. *Int. J. Pharm.* **241**, 47–55 (2002).
45. Fabiano, A., Bizzarri, R. & Zambito, Y. Thermosensitive hydrogel based on chitosan and its derivatives containing medicated nanoparticles for transcorneal administration of 5-fluorouracil. *Int. J. Nanomedicine* **12**, 633–643 (2017).
46. Morsi, N., Ibrahim, M., Refai, H. & El Sorogy, H. Nanoemulsion-based electrolyte triggered in situ gel for ocular delivery of acetazolamide. *Eur. J. Pharm. Sci.* **104**, 302–314 (2017).
47. Abu Hashim, I. I., El-dahan, M. S., Yusif, R. M., Abd-ElGawad, A.-E. H. & Arima, H. Potential Use of Niosomal Hydrogel as an Ocular Delivery System for Atenolol. *Biol. Pharm. Bull.* **37**, 541–551 (2014).
48. Yu, S. *et al.* Liposome incorporated ion sensitive in situ gels for opthalmic delivery of timolol maleate. *Int. J. Pharm.* **480**, 128–136 (2015).
49. Lux, A. A comparative bioavailability study of three conventional eye drops versus a single lyophilisate. *Br. J. Ophthalmol.* **87**, 436–440 (2003).
50. Shen, J., Wang, Y., Ping, Q., Xiao, Y. & Huang, X. Mucoadhesive effect of thiolated PEG stearate and its modified NLC for ocular drug delivery. *J. Controlled Release* **137**, 217–223 (2009).
51. Liu, D. *et al.* Potential advantages of a novel chitosan-N-acetylcysteine surface modified nanostructured lipid carrier on the performance of ophthalmic delivery of curcumin. *Sci. Rep.* **6**, 1–14 (2016).
52. Chanburee, S. & Tiyaboonchai, W. Mucoadhesive nanostructured lipid carriers (NLCs) as potential carriers for improving oral delivery of curcumin. *Drug Dev. Ind. Pharm.* **43**, 432–440 (2017).
53. Budai-Szűcs, M. *et al.* Mucoadhesive Cyclodextrin-Modified Thiolated Poly(aspartic acid) as a Potential Ophthalmic Drug Delivery System. *Polymers* **10**, 199 (2018).
54. Loftsson, T. & Stefánsson, E. Cyclodextrins in eye drop formulations: enhanced topical delivery of corticosteroids to the eye. *Acta Ophthalmol. Scand.* **80**, 144–150.
55. L. Kiss, E. *et al.* Design and Optimization of Nanostructured Lipid Carrier Containing Dexamethasone for Ophthalmic Use. *Pharmaceutics* **11**, 679 (2019).
56. Kiss, E. L. *et al.* Development and Characterization of Potential Ocular Mucoadhesive Nano Lipid Carriers Using Full Factorial Design. *Pharmaceutics* **12**, 682 (2020).
57. Araki-Sasaki, K. *et al.* An SV40-Immortalized Human Corneal Epithelial Cell Line and Its Characterization. *Investig. Ophthalmol. Vis. Sci. March* **36**, 614–621 (1995).
58. Woertz, C., Preis, M., Breitkreutz, J. & Kleinebudde, P. Assessment of test methods evaluating mucoadhesive polymers and dosage forms: An overview. *Eur. J. Pharm. Biopharm.* **85**, 843–853 (2013).
59. Horvát, G. *et al.* Thiolated poly(aspartic acid) as potential in situ gelling, ocular mucoadhesive drug delivery system. *Eur. J. Pharm. Sci.* **67**, 1–11 (2015).
60. Dargó, G. *et al.* Corneal-PAMPA: A novel, non-cell-based assay for prediction of corneal drug permeability. *Eur. J. Pharm. Sci.* **128**, 232–239 (2019).
61. Bocsik, A. *et al.* Dual Action of the PN159/KLAL/MAP Peptide: Increase of Drug Penetration across Caco-2 Intestinal Barrier Model by Modulation of Tight Junctions and Plasma Membrane Permeability. *Pharmaceutics* **11**, 73 (2019).
62. Loftsson, T., Jarho, P., Másson, M. & Järvinen, T. Cyclodextrins in drug delivery. *Expert Opin. Drug Deliv.* **2**, 335–351 (2005).
63. Castillo, J. A. *et al.* Preparation and Characterization of Albendazole β-Cyclodextrin Complexes. *Drug Dev. Ind. Pharm.* **25**, 1241–1248 (1999).
64. Ludwig, A. The use of mucoadhesive polymers in ocular drug delivery. *Adv. Drug Deliv. Rev.* **57**, 1595–1639 (2005).

65. Budai-Szűcs, M. *et al.* Cationic Thiolated Poly(aspartamide) Polymer as a Potential Excipient for Artificial Tear Formulations. *J. Ophthalmol.* **2016**, 1–8 (2016).
66. Patel, S., Boyd, K. E. & Burns, J. Age, stability of the precorneal tear film and the refractive index of tears. *Contact Lens Anterior Eye J. Br. Contact Lens Assoc.* **23**, 44–47 (2000).
67. Yañez-Soto, B. *et al.* Interfacial phenomena and the ocular surface. *Ocul. Surf.* **12**, 178–201 (2014).
68. Szilágyi, B. Á. *et al.* The effect of thiol content on the gelation and mucoadhesion of thiolated poly(aspartic acid). *Polym. Int.* **66**, 1538–1545 (2017).
69. Budai-Szűcs, M. *et al.* The effect of the antioxidant on the properties of thiolated poly(aspartic acid) polymers in aqueous ocular formulations. *Eur. J. Pharm. Biopharm.* **113**, 178–187 (2017).
70. Wright, P., Cooper, M. & Gilvarry, A. M. Effect of osmolarity of artificial tear drops on relief of dry eye symptoms: BJ6 and beyond. *Br. J. Ophthalmol.* **71**, 161–164 (1987).
71. Januleviciene, I., Siaudvytyte, L. & Barsauskaite, R. Ophthalmic Drug Delivery in Glaucoma—A Review. *Pharmaceutics* **4**, 243–251 (2012).
72. Peters, M. C. C. *et al.* Advances in ophthalmic preparation: the role of drug nanocrystals and lipid-based nanosystems. *J. Drug Target.* 1–12 (2019) doi:10.1080/1061186X.2019.1663858.
73. Coefficients table for Analyze Factorial Design. https://support.minitab.com/en-us/minitab/18/help-and-how-to/modeling-statistics/doe/how-to/factorial/analyze-factorial-design/interpret-the-results/all-statistics-and-graphs/coefficients-table/.
74. Siepmann, J. Modeling of drug release from delivery systems based on hydroxypropyl methylcellulose (HPMC). *Adv. Drug Deliv. Rev.* **48**, 139–157 (2001).
75. Andres-Guerrero, V. *et al.* The Use of Mucoadhesive Polymers to Enhance the Hypotensive Effect of a Melatonin Analogue, 5-MCA-NAT, in Rabbit Eyes. *Invest. Ophthalmol. Vis. Sci.* **52**, 1507–1515 (2011).
76. Schulz, M. B. & Daniels, R. Hydroxypropylmethylcellulose (HPMC) as emulsifier for submicron emulsions: influence of molecular weight and substitution type on the droplet size after high-pressure homogenization. *Eur. J. Pharm. Biopharm.* **49**, 231–236 (2000).
77. Kürti, L. *et al.* The effect of sucrose esters on a culture model of the nasal barrier. *Toxicol. In Vitro* **26**, 445–454 (2012).
78. Kiss, L. *et al.* Kinetic Analysis of the Toxicity of Pharmaceutical Excipients Cremophor EL and RH40 on Endothelial and Epithelial Cells. *J. Pharm. Sci.* **102**, 1173–1181 (2013).
79. Harazin, A. *et al.* Protection of cultured brain endothelial cells from cytokine-induced damage by α-melanocyte stimulating hormone. *PeerJ* **6**, (2018).
80. Kadmiel, M., Janoshazi, A., Xu, X. & Cidlowski, J. A. Glucocorticoid action in human corneal epithelial cells establishes roles for corticosteroids in wound healing and barrier function of the eye. *Exp. Eye Res.* **152**, 10–33 (2016).
81. Neuhaus, W. *et al.* Lung endothelial cells strengthen, but brain endothelial cells weaken barrier properties of a human alveolar epithelium cell culture model. *Differentiation* **84**, 294–304 (2012).
82. Mukaka, M. M. Statistics Corner: A guide to appropriate use of Correlation coefficient in medical research. *Malawi Med. J.* **24**, 69–71 (2012).
83. Tian, B.-C. *et al.* Further investigation of nanostructured lipid carriers as an ocular delivery system: in vivo transcorneal mechanism and in vitro release study. *Colloids Surf. B Biointerfaces* **102**, 251–256 (2013).

8. ACKNOWLEDGEMENTS

I would like to express my sincere gratitude to the Head of the Institute of Pharmaceutical Technology and Regulatory Affairs Prof. Dr. Ildikó Csóka for providing me with the opportunity to work in this Department and complete my Ph.D. work under her expert guidance.

I would like to express my warmest thanks to my supervisors Dr. habil. Erzsébet Csányi associate professor and Dr. habil. Mária Budai-Szűcs assistant professor for their guidance, patience, motivation and continuous support of my research.

I wish to thank Dr. Attila Gácsi for his immense help and co-operation, especially in HPLC measurements.

I wish to thank Dr. András Szilágyi, Dr. Benjamin Gyarmati, Barnabás Áron Szilágyi from Soft Matters Group, Department of Physical Chemistry and Materials Science, Budapest University of Technology and Economics for co-operation and synthetizing the thiolated polymers.

I wish to thank Dr. habil. György Tibor Balogh DSc. from Institute of Pharmacodynamics and Biopharmacy, Faculty of Pharmacy, University of Szeged and Department of Chemical and Environmental Process Engineering, Budapest University of Technology and Economics for co-operation in corneal-PAMPA measurements.

I owe many thanks to Judit Soós for his professional guidance on ophthalmic diseases.

I am very grateful to all my co-authors, Dr. habil. Mária A. Deli DSc., Dr. András Harazin, Ilona Gróf from Institute of Biophysics, Biological Research Centre, their immense help with the cell-line studies.

I am deeply indebted to the members of the second research group of the Institute of Pharmaceutical Technology and Regulatory Affairs.

I wish to thank all members of the Institute of Pharmaceutical Technology and Regulatory Affairs for their help and friendship.

I also owe a very important debt to my family and friends for their encouragement, support and understanding; and for ensuring a peaceful background.

NYILATKOZAT SAJÁT MUNKÁRÓL

Név: Dr. L.Kiss Eszter

A doktori értekezés címe: Increasing the ophthalmic bioavailability using innovative drug delivery systems

Én, Dr. L.Kiss Eszter teljes felelősségem tudatában kijelentem, hogy a Szegedi Tudományegyetem Gyógyszertudományok Doktori Iskolában elkészített doktori (Ph.D.) disszertációm saját kutatási eredményeimre alapulnak. Kutatómunkám, eredményeim publikálása, valamint disszertációm megírása során a Magyar Tudományos Akadémia Tudományetikai Kódexében lefektetett alapelvek és ajánlások szerint jártam el.

Szeged, 2021. 03. 04

dr. L. Kiss Eszter